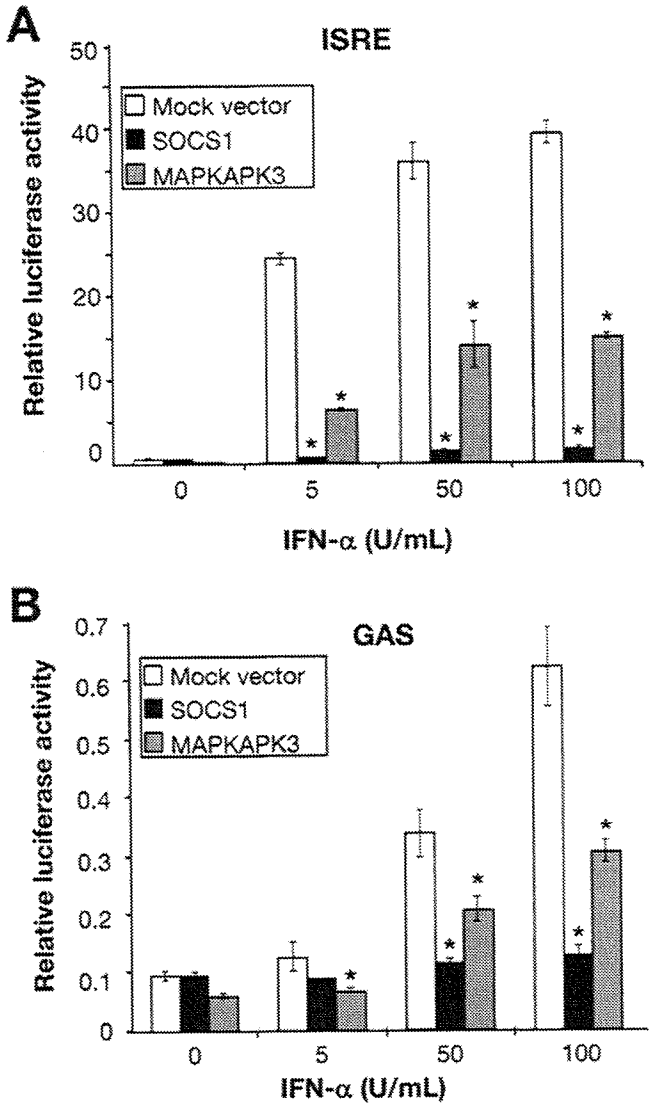

Figure 2. Effects of *MAPKAPK3* on IFN-α–induced gene transcription via ISRE and GAS elements. Huh7 cells were transfected with both 1 ng renilla luciferase expression vector pRL-TK (internal control) and 10 ng firefly luciferase expression vector (*A*) pISRE-TA-Luc or (*B*) pGAS-TA-Luc, in conjunction with 40 ng expression plasmid pDEST51/mock (negative control, *open bar*), pDEST51/suppressor of cytokine signaling 1 (SOCS1) (positive control, *black bar*), or pDEST51/*MAPKAPK3* (*gray bar*). After 24 hours, cells were stimulated with IFN-alfa for another 20 hours, and luciferase induction was measured. Firefly luciferase activity was normalized by renilla luciferase activity. Data represent the mean ± SD of triplicate assay. *$P < .05$ for comparison with mock.

with the outcome of IFN therapy in patients infected with HCV genotype 1b (Tables 2–4). In our genotype data of 1055 patients, the 2 SNPs were in strong linkage disequilibrium with an r^2 value of 0.82. Multivariate logistic regression analysis showed that rs3792323 is an independent factor associated with IFN efficacy (Table 4).

MAPKAPK3 is expressed in every human tissue.[38] *MAPKAPK3* encodes a serine/threonine-specific protein kinase and functions as a mitogen-activated protein kinase-activated protein kinase in both mitogen and stress responses.[39] MAPKAPK3 shares 72% nucleotide and 75% amino acid identity with MAPKAPK2. MAPKAPK3 and MAPKAPK2 act as downstream kinases of p38 MAP kinase under type I IFN stimulation.[22] It has been shown that disruption of p38α MAP kinase gene results in defective transcription of genes that are regulated by ISRE and GAS elements.[22] It also was reported that pharmacologic inhibition of p38 MAP kinase partially inhibits type I IFN–induced antiviral activity.[21] In mouse embryonic fibroblasts with targeted disruption of MAPKAPK2, it was indicated that type I IFN-induced antiviral activity was decreased.[22] On the other hand, little is known about the role of MAPKAPK3 in the responses to type I IFN.

In the present study, we hypothesized that enhanced expression of MAPKAPK3 is associated with resistance to IFN therapy for the following 3 reasons. First, carriers of the T allele for rs3792323, rather than the A allele, were more likely to show no response to IFN therapy (Tables 2 and 4). Thus, the T allele for rs3792323 was considered as a risk allele for nonresponse. Similarly, the A allele for rs616589 also was considered as a risk allele for nonresponse. Second, allele-specific *MAPKAPK3* mRNA expression corresponding to the T allele for rs3792323 (risk allele for nonresponse) was significantly higher than that of the A allele for rs3792323 in liver biopsy specimens of participating patients (Figure 1). Third, we did not find any nonsynonymous allelic variants in *MAPKAPK3* from the analysis of genomic DNA from 48 patients.

To examine our hypothesis, we examined whether enhanced MAPKAPK3 expression influences IFN-alfa–induced gene transcription. In reporter gene assay, overexpression of MAPKAPK3 inhibited IFN-alfa–induced gene transcription via ISRE and GAS elements (Figure 2), suggesting that MAPKAPK3 plays an important role in inhibition of IFN-α–induced antiviral activity. Several downstream effectors of MAPKAPK3 have been reported, including actin-binding protein, such as heat shock protein 27,[39] and transcription factors such as basic helix-loop-helix transcription factor E47[40] and cyclic AMP responsive element binding protein.[41] However, the mechanisms by which MAPKAPK3 inhibits IFN-α–induced gene transcription still are unclear, and further investigations are required. It also is interesting to examine the allele-specific *MAPKAPK3* mRNA levels during interferon therapy. Although we have no direct information, MAPKAKP3 mRNA expression is not inducible by IFN-alfa stimulation in human hepatoma cell line Huh-7 and HepG2 (data not shown).

In this study, the association between the *MAPKAPK3* polymorphisms and the efficacy of IFN therapy was observed in HCV genotype 1b, but not found in genotype non-1b. The reason for this difference between the 2 groups is yet to be seen. As one possible reason, the high susceptibility of genotype non-1b to IFN treatment may make the fine effect of SNPs obscure. As another possible

explanation, the effect of MAPKAPK3 on IFN efficacy may vary among different HCV genotypes. It was reported that associations between SNPs in the osteopontin gene and the efficacy of IFN therapy were particularly evident in patients with genotype 1b and a high virus titer, rather than in patients with genotype non-1b.[26] Until now, in various HCV genotypes including 1a, 1b, and 2a, HCV subgenomic replicon cell lines, which show autonomous HCV-RNA replication in the human hepatoma cell line, have been established. In the case that MAPKAPK3 is overexpressed in these HCV replicon cell lines, it is interesting to examine whether the effect of MAPKAPK3 on IFN efficacy is different or not among these HCV genotypes. It also is important to test associations between the *MAPKAPK3* SNPs and the IFN efficacy in each subgroup of patients infected with each HCV genotype including 1a, 2a, and 2b.

Recently, it was reported that the combination treatment of IFN-alfa plus ribavirin results in higher rates of sustained response than IFN monotherapy.[2,3] Various mechanisms of ribavirin activity against HCV have been proposed.[42] However, it is notable that treatment with ribavirin alone has no effect on serum HCV-RNA level.[43,44] On the other hand, the addition of ribavirin to IFN-alfa monotherapy leads to marked reduction of the serum HCV-RNA level. These facts suggest that IFN-alfa signaling is important for the induction of antiviral activity not only in IFN-alfa monotherapy but also in IFN-alfa combination therapy with ribavirin. Therefore, it is likely that the inhibitory effect of MAPKAPK3 on IFN signaling influences the efficacy of IFN-alfa combination therapy as well as IFN-alfa monotherapy. At present, about 50% of patients infected with HCV genotype 1b fail to eradicate the virus even after combination therapy of IFN-α plus ribavirin.[1-3] It is important to examine whether the 2 SNPs are associated with the responsiveness to combination therapy of IFN-alfa plus ribavirin.

It remains to be seen whether or not rs3792323 and rs616589 are functional cis-acting polymorphisms affecting *MAPKAPK3* expression. Even if the 2 SNPs do not have functional effects, it is expected that the 2 SNPs can serve as marker SNPs in linkage disequilibrium with functional cis-acting polymorphisms.[45] Furthermore, the 2 SNPs may be useful as genetic markers to predict the efficacy of IFN therapy. In our patients with IFN-alfa monotherapy, patients with risk alleles for nonresponse (T allele for rs3792323, A allele for rs616589) were more likely to be NRs compared with risk allele–negative patients (Tables 2 and 4). Although the results of our internal validation suggest that the observed association between the 2 SNPs in *MAPKAPK3* and the IFN efficacy is internally consistent, further replication with an independent cohort is needed to confirm the association. It also is interesting to test associations between the 2 SNPs and the phenotypes in relapsed patients. At present, we do not enroll enough of these patients to examine the association. In the future, we will enroll enough patients and test the association.

It was reported that polymorphism of GT-repeat length in the IFNAR1 promoter region was associated with the outcome of IFN therapy for chronic HCV infection in a study of 157 Japanese patients (HCV genotype total, $P = .008$).[13] In our study, we could not find a similar association for analyzed tagging-SNPs in IFNAR1 (Supplementary Table 2). The reason for the discrepancy between the 2 studies is not clear at present. Unfortunately, the GT-repeat polymorphism in IFNAR1 is not included in the HapMap database. Therefore, it is not clear whether tagging-SNPs have strong linkage disequilibrium with the GT-repeat polymorphism in IFNAR1. Possibly, tagging-SNPs may not capture the GT-repeat polymorphism in IFNAR1. To explain the discrepancy between the present study and the previous study, it is desirable to genotype the GT-repeat polymorphism in IFNAR1 by direct sequencing.

In conclusion, we identified that SNP rs3792323 in *MAPKAPK3* is associated strongly with the outcome of IFN therapy in patients infected with HCV genotype 1b. In addition, we showed that SNP rs3792323 associates with the expression level of *MAPKAPK3* and *MAPKAPK3* inhibits IFN-alfa–induced gene transcription via ISRE and GAS elements. Therefore, MAPKAPK3 may play an important role in the inhibition of IFN-alfa–induced antiviral activity.

Supplementary Data

Note: To access the supplementary material accompanying this article, visit the online version of *Gastroenterology* at www.gastrojournal.org, and at doi: 10.1053/j.gastro.2009.01.061.

Appendix

The authors thank the other members of the SNP Research Center for assistance with various aspects of this study.

Hiroshima Liver Study Group

Dr Tsuge and Dr Chayama are members of the Hiroshima Liver Study Group. Other members (listed in alphabetical order) include Hiroshi Aikata (Hiroshima University, Hiroshima, Japan), Shiomi Aimitsu (Hiroshima Red Cross Hospital, Hiroshima, Japan), Yasuyuki Aisaka (Hiroshima Red Cross Hospital, Hiroshima, Japan), Hajime Amano (Onomichi General Hospital, Hiroshima, Japan), Tatsuya Amimoto (Amimoto Clinic, Hiroshima, Japan), Keiko Arataki (Hiroshimakinen Hospital, Hiroshima, Japan), Nobuyuki Asada (Asada Clinic, Hiroshima, Japan), Takahiro Azakami (Hiroshima University, Hiroshima, Japan), Nobuhiko Hiraga (Hiroshima University, Hiroshima, Japan), Akira Hiramatsu (Chuden Hospital, Hiroshima, Japan), Hideyuki Hyogo (Hiroshima

University, Hiroshima, Japan), Michio Imamura (Hiroshima University, Hiroshima, Japan), Kunio Ishida (Hiroshima General Hospital, Hiroshima, Japan), Hiroto Ishihara (Chuden Hospital, Hiroshima, Japan), Tomokazu Ishitobi (Hiroshima University, Hiroshima, Japan), Hiroyuki Ito (Saiseikai Kure Hospital, Hiroshima, Japan), Keiko Iwamoto (Hiroshima University, Hiroshima, Japan), Soo Cheol Jeong (Hiroshima University, Hiroshima, Japan), Koji Kamada (Shobara Red Cross Hospital, Hiroshima, Japan), Masaya Kamiyasu (Kamiyasu Clinic, Hiroshima, Japan), Yoshio Katamura (Hiroshima University, Hiroshima, Japan), Hiroiku Kawakami (Kawakami Clinic, Hiroshima, Japan), Yoshiiku Kawakami (Hiroshima University, Hiroshima, Japan), Masahiro Kawanishi (Higashihiroshima Medical Center, Hiroshima, Japan), Tomokazu Kawaoka (Hiroshima University, Hiroshima, Japan), Takashi Kimura (Hiroshima University, Hiroshima, Japan), Shinsuke Kira (Hiroshima Red Cross Hospital, Hiroshima, Japan), Mikiya Kitamoto (Hiroshima Prefectural Hospital, Hiroshima, Japan), Hideaki Kodama (Saiseikai Hiroshima Hospital, Hiroshima, Japan), Hiroshi Kohno (Kure Medical Center, Hiroshima, Japan), Hirotaka Kohno (Kure Medical Center, Hiroshima, Japan), Toshiyuki Masanaga (Masanaga Clinic, Hiroshima, Japan), Akiko Matsumoto (Hiroshima Mitsubishi Hospital, Hiroshima, Japan), Daiki Miki (Hiroshima University, Hiroshima, Japan), Fukiko Mitsui (Hiroshima University, Hiroshima, Japan), Toshio Miura (Akitsu Prefectural Hospital, Hiroshima, Japan), Nami Mori (Hiroshima University, Hiroshima, Japan), Takashi Moriya (Chugoku Rousai Hospital, Hiroshima, Japan), Yutaka Nabeshima (Hiroshima University, Hiroshima, Japan), Toshio Nakamura (Nakamura Clinic, Hiroshima, Japan), Toshio Nakanishi (Shobara Red Cross Hospital, Hiroshima, Japan), Ryo Nakashio (Nakashio Clinic, Hiroshima, Japan), Michihiro Nanaka (Hiroshima University, Hiroshima, Japan), Makoto Ohbayashi (Onomichi General Hospital, Hiroshima, Japan), Waka Ohishi (Radiation Effects Research Foundation, Hiroshima, Japan), Shigeo Orime (Chuden Hospital, Hiroshima, Japan), Hiromi Saneto (Hiroshima University, Hiroshima, Japan), Hiroo Shirakawa (Funairi Hospital, Hiroshima, Japan), Shoichi Takahashi (Hiroshima University, Hiroshima, Japan), Shintaro Takaki (Hiroshima University, Hiroshima, Japan), Eichi Takesaki (Higashihiroshima Medical Center, Hiroshima, Japan), Toru Tamura (Mazda Hospital, Hiroshima, Japan), Keiji Tsuji (Hiroshima City Asa Hospital, Hiroshima, Japan), Kiminori Uka (Hiroshima University, Hiroshima, Japan), Koji Waki (Saiseikai Hiroshima Hospital, Hiroshima, Japan), Masashi Watanabe (Kuchiwa Clinic, Hiroshima, Japan), Syuji Yamaguchi (Kure Kyosai Hospital, Hiroshima, Japan), Keitaro Yamashina (Hiroshima General Hospital of West Japan Railway Company, Hiroshima, Japan), Hitoshi Yokoya (Fuchu Kita Hospital, Hiroshima, Japan), and Tatsuji Yokoyama (Takanobashi Central Hospital, Hiroshima, Japan).

Toranomon Hospital

Dr Kumada is a member of the Department of Hepatology, Toranomon Hospital. Other members (listed in alphabetical order) include Norio Akuta, Yasuji Arase, Miharu Hirakawa, Tetsuya Hosaka, Kenji Ikeda, Yusuke Kawamura, Mariko Kobayashi, Masahiro Kobayashi, Satoshi Saitoh, Hitomi Sezaki, Yoshiyuki Suzuki, Fumitaka Suzuki, and Hiromi Yatsuji.

References

1. Fried MW, Shiffman ML, Reddy KR, et al. Peginterferon alfa-2a plus ribavirin for chronic hepatitis C virus infection. N Engl J Med 2002;347:975–982.
2. Management of hepatitis C. NIH Consensus Statement 1997; available at http://consensus.nih.gov/1997/1997HepatitisC105html.htm.
3. Liang TJ, Rehermann B, Seeff LB, et al. Pathogenesis, natural history, treatment, and prevention of hepatitis C. Ann Intern Med 2000;132:296–305.
4. Martinot-Peignoux M, Marcellin P, Pouteau M, et al. Pretreatment serum hepatitis C virus RNA levels and hepatitis C virus genotype are the main and independent prognostic factors of sustained response to interferon alfa therapy in chronic hepatitis C. Hepatology 1995;22:1050–1056.
5. Trepo C. Genotype and viral load as prognostic indicators in the treatment of hepatitis C. J Viral Hepat 2000;7:250–257.
6. Walsh MJ, Jonsson JR, Richardson MM, et al. Non-response to antiviral therapy is associated with obesity and increased hepatic expression of suppressor of cytokine signalling 3 (SOCS-3) in patients with chronic hepatitis C, viral genotype 1. Gut 2006;55:529–535.
7. Gao B, Hong F, Radaeva S. Host factors and failure of interferon-alpha treatment in hepatitis C virus. Hepatology 2004;39:880–890.
8. Huang Y, Yang H, Borg BB, et al. A functional SNP of interferon-gamma gene is important for interferon-alpha-induced and spontaneous recovery from hepatitis C virus infection. Proc Natl Acad Sci U S A 2007;104:985–990.
9. Yee LJ, Tang J, Gibson AW, et al. Interleukin 10 polymorphisms as predictors of sustained response in antiviral therapy for chronic hepatitis C infection. Hepatology 2001;33:708–712.
10. Naito M, Matsui A, Inao M, et al. SNPs in the promoter region of the osteopontin gene as a marker predicting the efficacy of interferon-based therapies in patients with chronic hepatitis C. J Gastroenterol 2005;40:381–388.
11. Suzuki F, Arase Y, Suzuki Y, et al. Single nucleotide polymorphism of the MxA gene promoter influences the response to interferon monotherapy in patients with hepatitis C viral infection. J Viral Hepat 2004;11:271–276.
12. Vidigal PG, Germer JJ, Zein NN. Polymorphisms in the interleukin-10, tumor necrosis factor-alpha, and transforming growth factor-beta1 genes in chronic hepatitis C patients treated with interferon and ribavirin. J Hepatol 2002;36:271–277.
13. Matsuyama N, Mishiro S, Sugimoto M, et al. The dinucleotide microsatellite polymorphism of the IFNAR1 gene promoter correlates with responsiveness of hepatitis C patients to interferon. Hepatol Res 2003;25:221–225.
14. Pharoah PD, Dunning AM, Ponder BA, et al. Association studies for finding cancer-susceptibility genetic variants. Nat Rev Cancer 2004;4:850–860.

15. Johnson GC, Esposito L, Barratt BJ, et al. Haplotype tagging for the identification of common disease genes. Nat Genet 2001; 29:233–237.
16. Gibbs RA, Belmont JW, Hardenbol P, et al. The International HapMap Project. Nature 2003;426:789–796.
17. Darnell JE Jr, Kerr IM, Stark GR. Jak-STAT pathways and transcriptional activation in response to IFNs and other extracellular signaling proteins. Science 1994;264:1415–1421.
18. Uddin S, Lekmine F, Sharma N, et al. The Rac1/p38 mitogen-activated protein kinase pathway is required for interferon alpha-dependent transcriptional activation but not serine phosphorylation of Stat proteins. J Biol Chem 2000;275:27634–27640.
19. Li Y, Batra S, Sassano A, et al. Activation of mitogen-activated protein kinase kinase (MKK) 3 and MKK6 by type I interferons. J Biol Chem 2005;280:10001–10010.
20. Uddin S, Majchrzak B, Woodson J, et al. Activation of the p38 mitogen-activated protein kinase by type I interferons. J Biol Chem 1999;274:30127–30131.
21. Mayer IA, Verma A, Grumbach IM, et al. The p38 MAPK pathway mediates the growth inhibitory effects of interferon-alpha in BCR-ABL-expressing cells. J Biol Chem 2001;276:28570–28577.
22. Li Y, Sassano A, Majchrzak B, et al. Role of p38alpha Map kinase in type I interferon signaling. J Biol Chem 2004;279:970–979.
23. Ishida H, Ohkawa K, Hosui A, et al. Involvement of p38 signaling pathway in interferon-alpha-mediated antiviral activity toward hepatitis C virus. Biochem Biophys Res Commun 2004;321:722–727.
24. Hoofnagle JH. Therapy of acute and chronic viral hepatitis. Adv Intern Med 1994;39:241–275.
25. Shiratori Y, Kato N, Yokosuka O, et al. Predictors of the efficacy of interferon therapy in chronic hepatitis C virus infection. Tokyo-Chiba Hepatitis Research Group. Gastroenterology 1997;113: 558–566.
26. Naito M, Matsui A, Inao M, et al. SNPs in the promoter region of the osteopontin gene as a marker predicting the efficacy of interferon-based therapies in patients with chronic hepatitis C. J Gastroenterol 2005;40:381–388.
27. Desmet VJ, Gerber M, Hoofnagle JH, et al. Classification of chronic hepatitis: diagnosis, grading and staging. Hepatology 1994;19:1513–1520.
28. Ozaki K, Ohnishi Y, Iida A, et al. Functional SNPs in the lymphotoxin-alpha gene that are associated with susceptibility to myocardial infarction. Nat Genet 2002;32:650–654.
29. Ohnishi Y, Tanaka T, Ozaki K, et al. A high-throughput SNP typing system for genome-wide association studies. J Hum Genet 2001; 46:471–477.
30. Suzuki A, Yamada R, Chang X, et al. Functional haplotypes of PADI4, encoding citrullinating enzyme peptidylarginine deiminase 4, are associated with rheumatoid arthritis. Nat Genet 2003;34: 395–402.
31. Iida A, Saito S, Sekine A, et al. Catalog of 258 single-nucleotide polymorphisms (SNPs) in genes encoding three organic anion transporters, three organic anion-transporting polypeptides, and three NADH:ubiquinone oxidoreductase flavoproteins. J Hum Genet 2001;46:668–683.
32. Osawa N, Koya D, Araki S, et al. Combinational effect of genes for the renin-angiotensin system in conferring susceptibility to diabetic nephropathy. J Hum Genet 2007;52:143–151.
33. Kamiyama M, Kobayashi M, Araki SI, et al. Polymorphisms in the 3′ untranslated region in the neurocalcin delta gene affect mRNA stability, and confer susceptibility to diabetic nephropathy. Hum Genet 2007;122:397–407.
34. Nielsen DM, Ehm MG, Weir BS. Detecting marker-disease association by testing for Hardy-Weinberg disequilibrium at a marker locus. Am J Hum Genet 1998;63:1531–1540.
35. Sladek R, Rocheleau G, Rung J, et al. A genome-wide association study identifies novel risk loci for type 2 diabetes. Nature 2007; 445:881–885.
36. Devlin B, Risch N. A comparison of linkage disequilibrium measures for fine-scale mapping. Genomics 1995;29:311–322.
37. Freedman ML, Reich D, Penney KL, et al. Assessing the impact of population stratification on genetic association studies. Nat Genet 2004;36:388–393.
38. Sithanandam G, Latif F, Duh FM, et al. 3pK, a new mitogen-activated protein kinase-activated protein kinase located in the small cell lung cancer tumor suppressor gene region. Mol Cell Biol 1996;16:868–876.
39. Ludwig S, Engel K, Hoffmeyer A, et al. 3pK, a novel mitogen-activated protein (MAP) kinase-activated protein kinase, is targeted by three MAP kinase pathways. Mol Cell Biol 1996;16: 6687–6697.
40. Neufeld B, Grosse-Wilde A, Hoffmeyer A, et al. Serine/threonine kinases 3pK and MAPK-activated protein kinase 2 interact with the basic helix-loop-helix transcription factor E47 and repress its transcriptional activity. J Biol Chem 2000;275:20239–20242.
41. Maizels ET, Mukherjee A, Sithanandam G, et al. Developmental regulation of mitogen-activated protein kinase-activated kinases-2 and -3 (MAPKAPK-2/-3) in vivo during corpus luteum formation in the rat. Mol Endocrinol 2001;15:716–733.
42. Feld JJ, Hoofnagle JH. Mechanism of action of interferon and ribavirin in treatment of hepatitis C. Nature 2005;436:967–972.
43. Lau JY, Tam RC, Liang TJ, et al. Mechanism of action of ribavirin in the combination treatment of chronic HCV infection. Hepatology 2002;35:1002–1009.
44. Hoofnagle JH, Lau D, Conjeevaram H, et al. Prolonged therapy of chronic hepatitis C with ribavirin. J Viral Hepat 1996;3:247–252.
45. Gabriel SB, Schaffner SF, Nguyen H, et al. The structure of haplotype blocks in the human genome. Science 2002;296: 2225–2229.

Received January 03, 2008. Accepted January 29, 2009.

Reprint requests

Address requests for reprints to: Kazuaki Chayama, MD, PhD, Laboratory for Digestive Diseases, Center for Genomic Medicine, RIKEN (The Institute of Physical and Chemical Research), 1-2-3 Kasumi, Minami-ku, Hiroshima 734-8551, Japan. e-mail: chayama@hiroshima-u.ac.jp; fax: (81) 82-255-6220.

Acknowledgment

The authors thank the patients who generously agreed to participate in this study. The authors also thank the team members at the Department of Hepatology, Toranomon Hospital, Hiroshima University Hospital, and Hiroshima Liver Study Group for clinical sample collection. The authors acknowledge Dr N. Osawa and Dr Y. Nagasaka for helpful discussion; and Y. Kikuchi, M. Habata, M. Yahata, and T. Hirooka for technical assistance.

Conflicts of Interest

The authors disclose no conflicts.

Funding

This study was supported by a grant from the Japanese Millennium Project, and in part by Dainippon Sumitomo Pharma Co, Ltd. This work was also supported in part by a Grant-in-Aid for Scientific Research and Development from the Ministry of Education, Sports, Culture, and Technology and the Ministry of Health, Labor, and Welfare.

Supplementary Table 1. Candidate Genes Related to Type I IFN Pathway and Selected 116 Tagging-SNPs

dbSNP ID	Gene symbol	Alleles	SNP bin	SNP location
rs2243594	*IFNAR1*	A/G	Bin1	Intron2_108
rs2243600	*IFNAR1*	G/T	Bin2	Intron8_1812
rs2252930	*IFNAR1*	C/G	Bin3	Intron1_6765
rs2252650	*IFNAR2*	A/T	Bin1	Intron4_571
rs6517154	*IFNAR2*	T/C	Bin2	Intron1_6159
rs2073362	*IFNAR2*	A/G	Bin3	Intron5_1606
rs2248202	*IFNAR2*	A/C	Bin4	Intron1_1359
rs10211925	*IFNAR2*	G/A	Bin5	Intron2_1450
rs2248412	*IFNAR2*	A/G	Bin7	Intron1_3010
rs310209	*JAK1*	C/A	Bin1	Intron2_3344
rs3790541	*JAK1*	C/T	Bin2	Intron3_3141
rs310247	*JAK1*	A/G	Bin3	Intron16_2338
rs3790532	*JAK1*	G/A	Bin4	Intron21_225
rs2254002	*JAK1*	A/C	Bin5	Intron22_112
rs3818753	*JAK1*	A/G	Bin6	Intron3_5476
rs17127024	*JAK1*	G/T	Bin7	Intron21_484
rs2274948	*JAK1*	T/C	Bin8	Intron9_1930
rs280523	Tyrosine kinase2	G/A	Bin1	Exon6_51
rs280519	Tyrosine kinase2	A/G	Bin2	Intron11_7
rs280496	Tyrosine kinase2	C/G	Bin3	Intron22_122
rs11885069	*STAT1*	C/T	Bin1	Intron5_1665
rs9789428	*STAT1*	C/A	Bin2	Intron21_656
rs2280233	*STAT1*	T/C	Bin3	Intron14_1014
rs13395505	*STAT1*	A/G	Bin4	3′flank_1750
rs12693589	*STAT1*	C/T	Bin5	3′flank_7602
rs2066805	*STAT1*	T/C	Bin6	Intron8_42
rs1400657	*STAT1*	T/G	Bin7	3′flank_6724
rs3771300	*STAT1*	T/G	Bin8	3′flank_4668
rs11677408	*STAT1*	C/T	Bin9	Intron5_5674
rs11887698	*STAT1*	A/G	Bin10	Intron11_1080
rs2030171	*STAT1*	A/G	Bin11	Intron5_3126
rs1467199	*STAT1*	C/G	Bin12	5′flank_-1566
rs10199181	*STAT1*	T/A	Bin13	Intron4_136
rs2066802	*STAT1*	A/G	Bin15	Exon3_64
rs16833155	*STAT1*	C/T	Bin16	Intron9_1205
rs2066799	*STAT1*	C/T	Bin17	Intron14_95
rs11693463	*STAT1*	A/G	Bin18	Intron5_2378
rs10208033	*STAT1*	C/T	Bin19	5′flank_-481
rs3755312	*STAT1*	C/G	Bin20	Intron18_1118
rs2280232	*STAT1*	A/C	Bin21	Intron14_814
rs13029532	*STAT1*	A/C	Bin22	Intron2_2350
rs7562024	*STAT1*	T/C	Bin23	Intron11_433
rs1914408	*STAT1*	C/T	Bin24	3′flank_288
rs2066807	*STAT2*	C/G	Bin1	Exon20_58
rs12432194	IFN regulatory factor 9	C/T	Bin1	3′flank_251
rs4981494	IFN regulatory factor 9	G/A	Bin2	5′flank_-331
rs12432304	IFN regulatory factor 9	C/T	Bin3	3′flank_1029
rs2277484	IFN regulatory factor 9	G/A	Bin4	5′flank_-678
rs2236350	IFN regulatory factor 9	C/A	Bin5	Intron1_463
rs2303364	Ras-related C3 botulinum toxin substrate 1	C/T	Bin1	Intron6_30
rs836483	Ras-related C3 botulinum toxin substrate 1	G/A	Bin2	Intron3_827
rs6954996	Ras-related C3 botulinum toxin substrate 1	G/A	Bin3	Intron5_1439
rs7456834	Ras-related C3 botulinum toxin substrate 1	G/C	Bin4	Intron2_1041
rs702484	Ras-related C3 botulinum toxin substrate 1	G/C	Bin5	Intron4_261
rs2347339	Ras-related C3 botulinum toxin substrate 1	C/G	Bin6	Intron2_8177
rs768409	Ras-related C3 botulinum toxin substrate 1	A/T	Bin7	Intron1_9471
rs2305871	*MAPKK3*	G/C	Bin1	Intron6_35
rs9901404	*MAPKK3*	G/A	Bin2	3′flank_5917
rs12602109	*MAPKK3*	G/A	Bin3	3′flank_8737
rs3760201	*MAPKK3*	A/G	Bin4	Intron1_5337
rs8074866	*MAPKK3*	C/T	Bin5	Intron1_2246
rs2074028	*MAPKK6*	T/C	Bin1	Intron7_308
rs2034100	*MAPKK6*	G/A	Bin2	Intron1_1022

Supplementary Table 1. (Continued)

dbSNP ID	Gene symbol	Alleles	SNP bin	SNP location
rs817565	*MAPKK6*	T/G	Bin3	Intron1_21244
rs2251862	*MAPKK6*	C/A	Bin4	Exon3_8
rs2072073	*MAPKK6*	C/G	Bin5	3'flank_500
rs2716213	*MAPKK6*	T/G	Bin6	Intron1_86422
rs12451722	*MAPKK6*	T/C	Bin7	Intron1_23084
rs6501326	*MAPKK6*	A/G	Bin8	Intron1_31727
rs2716225	*MAPKK6*	G/A	Bin9	Intron1_56816
rs8080760	*MAPKK6*	A/G	Bin10	Intron1_45400
rs12948059	*MAPKK6*	A/G	Bin11	Intron1_83353
rs2074027	*MAPKK6*	A/G	Bin12	Intron2_151
rs2716222	*MAPKK6*	C/T	Bin13	Intron1_75110
rs4968857	*MAPKK6*	T/C	Bin14	Intron1_9292
rs756944	*MAPKK6*	T/C	Bin15	Intron10_8385
rs2715806	*MAPKK6*	G/A	Bin16	Intron1_48526
rs8078890	*MAPKK6*	A/C	Bin17	Intron1_71173
rs2716191	*MAPKK6*	C/T	Bin18	Intron11_4021
rs2715812	*MAPKK6*	C/T	Bin19	Intron1_57430
rs11869073	*MAPKK6*	A/C	Bin20	Intron1_65672
rs12945375	*MAPKK6*	A/G	Bin21	Intron1_58307
rs12939509	*MAPKK6*	A/G	Bin22	Intron1_38245
rs8082399	*MAPKK6*	G/A	Bin23	Intron1_3166
rs2716195	*MAPKK6*	G/A	Bin24	Intron10_5581
rs2716223	*MAPKK6*	G/A	Bin25	Intron1_75080
rs2715810	*MAPKK6*	G/A	Bin26	Intron1_40643
rs7213686	*MAPKK6*	T/C	Bin27	Intron1_42333
rs8067307	*MAPKK6*	C/A	Bin28	Intron10_5994
rs4968859	*MAPKK6*	A/C	Bin29	Intron1_47927
rs9893349	*MAPKK6*	G/A	Bin30	Intron1_62870
rs17690015	*MAPKK6*	G/A	Bin31	Intron1_51658
rs2715834	*MAPKK6*	G/C	Bin32	Intron10_5872
rs1548444	*MAPKK6*	T/G	Bin33	Intron1_65966
rs2715817	*MAPKK6*	T/C	Bin34	Intron1_71609
rs2715832	*MAPKK6*	T/C	Bin35	Intron10_4665
rs7761118	p38 MAP kinase	G/A	Bin1	Intron9_4460
rs2145362	p38 MAP kinase	C/G	Bin2	Intron3_2031
rs3752525	p38 MAP kinase	G/T	Bin3	Intron10_245
rs3730326	p38 MAP kinase	G/T	Bin4	Intron5_210
rs7770710	p38 MAP kinase	C/T	Bin5	Intron2_2152
rs16884694	p38 MAP kinase	G/A	Bin6	Intron8_18777
rs13196204	p38 MAP kinase	T/G	Bin7	Intron1_2726
rs3804453	p38 MAP kinase	A/G	Bin8	Exon12_542
rs3804454	p38 MAP kinase	T/G	Bin9	Intron1_10948
rs10807156	p38 MAP kinase	A/T	Bin10	Intron1_8809
rs4844550	*MAPKAPK2*	A/G	Bin1	5'flank_-882
rs10863784	*MAPKAPK2*	C/G	Bin2	Intron1_12931
rs12028997	*MAPKAPK2*	C/T	Bin3	Intron1_23505
rs4073250	*MAPKAPK2*	C/T	Bin4	Exon8_59
rs4072677	*MAPKAPK2*	T/G	Bin5	Intron1_20269
rs12060808	*MAPKAPK2*	C/T	Bin7	Intron1_18484
rs616589	*MAPKAPK3*	G/A	Bin1	Intron2_8414
rs3792323	*MAPKAPK3*	A/T	Bin2	Intron2_5116
rs3804628	*MAPKAPK3*	G/A	Bin3	Intron2_6866
rs2040397	*MAPKAPK3*	C/T	Bin4	Intron2_14863

Supplementary Table 2. Genotyping Results of 116 Tagging-SNPs

SNP	Gene	Alleles (1/2)	Group	All patients with HCV infection: No. of genotypes (%) 1/1	1/2	2/2	Patients with HCV genotype 1b: No. of genotypes (%) 1/1	1/2	2/2
rs2243594	*IFNAR1*	A/G	SR	210 (45.1)	213 (45.7)	43 (9.2)	94 (50.3)	93 (49.7)	20 (10.7)
			NR	263 (45.2)	245 (42.1)	74 (12.7)	198 (50.3)	176 (44.7)	55 (14)
rs2243600	*IFNAR1*	G/T	SR	128 (27.5)	223 (47.9)	115 (24.7)	62 (30)	101 (48.8)	44 (21.3)
			NR	163 (28)	300 (51.5)	120 (20.6)	119 (27.7)	217 (50.5)	94 (21.9)
rs2252930	*IFNAR1*	C/G	SR	298 (63.8)	152 (32.5)	17 (3.6)	125 (60.1)	75 (36.1)	8 (3.8)
			NR	362 (62.2)	191 (32.8)	29 (5)	274 (63.9)	134 (31.2)	21 (4.9)
rs2252650	*IFNAR2*	A/T	SR	145 (31)	227 (48.6)	95 (20.3)	63 (30.4)	101 (48.8)	43 (20.8)
			NR	168 (28.7)	293 (50)	125 (21.3)	119 (27.5)	219 (50.6)	95 (21.9)
rs6517154	*IFNAR2*	T/C	SR	413 (88.6)	50 (10.7)	3 (0.6)	181 (87.4)	24 (11.6)	2 (1)
			NR	509 (86.9)	76 (13)	1 (0.2)	378 (87.3)	54 (12.5)	1 (0.2)
rs2073362	*IFNAR2*	A/G	SR	338 (73)	116 (25.1)	9 (1.9)	149 (72.7)	52 (25.4)	4 (2)
			NR	452 (77.4)	121 (20.7)	11 (1.9)	341 (79.1)	84 (19.5)	6 (1.4)
rs2248202	*IFNAR2*	A/C	SR	183 (39.4)	210 (45.3)	71 (15.3)	80 (39)	96 (46.8)	29 (14.1)
			NR	218 (37.2)	274 (46.8)	94 (16)	155 (35.8)	205 (47.3)	73 (16.9)
rs10211925	*IFNAR2*	G/A	SR	436 (94.4)	26 (5.6)	0 (0)	189 (91.7)	17 (8.3)	0 (0)
			NR	553 (95.2)	27 (4.6)	1 (0.2)	412 (95.6)	18 (4.2)	1 (0.2)
rs2248412	*IFNAR2*	A/G	SR	269 (57.5)	166 (35.5)	33 (7.1)	114 (54.8)	81 (38.9)	13 (6.3)
			NR	313 (53.4)	232 (39.6)	41 (7)	228 (52.5)	177 (40.8)	29 (6.7)
rs310209	*JAK1*	C/A	SR	240 (51.6)	182 (39.1)	43 (9.2)	109 (52.7)	76 (36.7)	22 (10.6)
			NR	293 (49.9)	251 (42.8)	43 (7.3)	208 (47.9)	190 (43.8)	36 (8.3)
rs3790541	*JAK1*	C/T	SR	239 (51.2)	189 (40.5)	39 (8.4)	99 (47.6)	85 (40.9)	24 (11.5)
			NR	295 (50.5)	245 (42)	44 (7.5)	220 (50.8)	177 (40.9)	36 (8.3)
rs310247	*JAK1*	A/G	SR	147 (31.5)	233 (49.9)	87 (18.6)	72 (34.6)	105 (50.5)	31 (14.9)
			NR	180 (30.8)	295 (50.5)	109 (18.7)	140 (32.4)	220 (50.9)	72 (16.7)
rs3790532	*JAK1*	G/A	SR	252 (54.3)	175 (37.7)	37 (8)	114 (55.3)	74 (35.9)	18 (8.7)
			NR	317 (54)	232 (39.5)	38 (6.5)	224 (51.6)	176 (40.6)	34 (7.8)
rs2254002	*JAK1*	A/C	SR	158 (33.8)	230 (49.1)	80 (17.1)	74 (35.6)	106 (51)	28 (13.5)
			NR	186 (31.7)	304 (51.8)	97 (16.5)	145 (33.4)	225 (51.8)	64 (14.7)
rs3818753	*JAK1*	A/G	SR	405 (86.5)	59 (12.6)	4 (0.9)	173 (83.2)	31 (14.9)	4 (1.9)
			NR	532 (90.9)	53 (9.1)	0 (0)	389 (89.8)	44 (10.2)	0 (0)
rs17127024	*JAK1*	G/T	SR	310 (66.4)	134 (28.7)	23 (4.9)	141 (67.8)	56 (26.9)	11 (5.3)
			NR	369 (62.9)	194 (33)	24 (4.1)	276 (63.6)	142 (32.7)	16 (3.7)
rs2274948	*JAK1*	T/C	SR	358 (77)	98 (21.1)	9 (1.9)	154 (74.8)	48 (23.3)	4 (1.9)
			NR	424 (72.9)	153 (26.3)	5 (0.9)	312 (72.2)	115 (26.6)	5 (1.2)
rs280523	Tyrosine kinase2	G/A	SR	416 (89.3)	47 (10.1)	3 (0.6)	182 (87.9)	25 (12.1)	0 (0)
			NR	520 (88.6)	66 (11.2)	1 (0.2)	387 (89.2)	46 (10.6)	1 (0.2)
rs280519	Tyrosine kinase2	A/G	SR	134 (28.8)	241 (51.7)	91 (19.5)	58 (27.9)	113 (54.3)	37 (17.8)
			NR	166 (28.4)	293 (50.1)	126 (21.5)	130 (30)	208 (48)	95 (21.9)
rs280496	Tyrosine kinase2	C/G	SR	391 (83.5)	75 (16)	2 (0.4)	172 (82.7)	36 (17.3)	0 (0)
			NR	485 (82.6)	96 (16.4)	6 (1)	360 (82.9)	69 (15.9)	5 (1.2)
rs11885069	*STAT1*	C/T	SR	363 (78.1)	93 (20)	9 (1.9)	155 (75.2)	46 (22.3)	5 (2.4)
			NR	466 (79.5)	115 (19.6)	5 (0.9)	335 (77.4)	94 (21.7)	4 (0.9)
rs9789428	*STAT1*	C/A	SR	415 (88.7)	51 (10.9)	2 (0.4)	182 (87.5)	24 (11.5)	2 (1)
			NR	523 (89.4)	61 (10.4)	1 (0.2)	384 (88.9)	47 (10.9)	1 (0.2)
rs2280233	*STAT1*	T/C	SR	339 (72.6)	124 (26.6)	4 (0.9)	161 (77.8)	45 (21.7)	1 (0.5)
			NR	444 (75.8)	133 (22.7)	9 (1.5)	331 (76.4)	95 (21.9)	7 (1.6)
rs13395505	*STAT1*	A/G	SR	173 (37)	216 (46.3)	78 (16.7)	88 (42.5)	86 (41.5)	33 (15.9)
			NR	227 (38.7)	269 (45.8)	91 (15.5)	172 (39.6)	195 (44.9)	67 (15.4)
rs12693589	*STAT1*	C/T	SR	130 (27.8)	229 (48.9)	109 (23.3)	69 (33.2)	91 (43.8)	48 (23.1)
			NR	164 (27.9)	301 (51.3)	122 (20.8)	124 (28.6)	221 (50.9)	89 (20.5)
rs2066805	*STAT1*	T/C	SR	436 (93.2)	32 (6.8)	0 (0)	197 (94.7)	11 (5.3)	0 (0)
			NR	533 (91)	51 (8.7)	2 (0.3)	395 (91.2)	36 (8.3)	2 (0.5)
rs1400657	*STAT1*	T/G	SR	356 (76.1)	100 (21.4)	12 (2.6)	170 (81.7)	35 (16.8)	3 (1.4)
			NR	441 (75.3)	129 (22)	16 (2.7)	338 (78.1)	85 (19.6)	10 (2.3)
rs3771300	*STAT1*	T/G	SR	246 (52.6)	185 (39.5)	37 (7.9)	110 (52.9)	78 (37.5)	20 (9.6)
			NR	327 (56.2)	216 (37.1)	39 (6.7)	236 (54.9)	163 (37.9)	31 (7.2)
rs11677408	*STAT1*	C/T	SR	393 (84.2)	70 (15)	4 (0.9)	170 (82.1)	35 (16.9)	2 (1)
			NR	500 (85.3)	82 (14)	4 (0.7)	361 (83.4)	69 (15.9)	3 (0.7)
rs11887698	*STAT1*	A/G	SR	260 (55.6)	171 (36.5)	37 (7.9)	110 (52.9)	80 (38.5)	18 (8.7)
			NR	344 (58.6)	217 (37)	26 (4.4)	245 (56.5)	167 (38.5)	22 (5.1)

Supplementary Table 2. (Continued)

SNP	Gene	Alleles (1/2)	Group	All patients with HCV infection: No. of genotypes (%) 1/1	1/2	2/2	Patients with HCV genotype 1b: No. of genotypes (%) 1/1	1/2	2/2
rs2030171	*STAT1*	A/G	SR	214 (46.1)	202 (43.5)	48 (10.3)	105 (51)	80 (38.8)	21 (10.2)
			NR	268 (45.9)	252 (43.2)	64 (11)	203 (47.1)	181 (42)	47 (10.9)
rs1467199	*STAT1*	C/G	SR	119 (25.6)	236 (50.9)	109 (23.5)	44 (21.5)	101 (49.3)	60 (29.3)
			NR	162 (27.9)	286 (49.2)	133 (22.9)	115 (26.7)	215 (50)	100 (23.3)
rs10199181	*STAT1*	T/A	SR	231 (49.4)	189 (40.4)	48 (10.3)	115 (55.3)	75 (36.1)	18 (8.7)
			NR	286 (48.9)	245 (41.9)	54 (9.2)	222 (51.3)	174 (40.2)	37 (8.5)
rs2066802	*STAT1*	A/G	SR	288 (62.5)	149 (32.3)	24 (5.2)	128 (63.7)	64 (31.8)	9 (4.5)
			NR	373 (64)	179 (30.7)	31 (5.3)	271 (63)	136 (31.6)	23 (5.3)
rs16833155	*STAT1*	C/T	SR	436 (93.4)	31 (6.6)	0 (0)	196 (94.7)	11 (5.3)	0 (0)
			NR	531 (91.1)	50 (8.6)	2 (0.3)	394 (91.4)	35 (8.1)	2 (0.5)
rs2066799	*STAT1*	C/T	SR	391 (83.5)	70 (15)	7 (1.5)	169 (81.3)	35 (16.8)	4 (1.9)
			NR	496 (84.6)	86 (14.7)	4 (0.7)	358 (82.7)	72 (16.6)	3 (0.7)
rs11693463	*STAT1*	A/G	SR	338 (72.4)	118 (25.3)	11 (2.4)	148 (71.5)	53 (25.6)	6 (2.9)
			NR	419 (71.6)	153 (26.2)	13 (2.2)	303 (70)	119 (27.5)	11 (2.5)
rs10208033	*STAT1*	C/T	SR	208 (44.5)	212 (45.4)	47 (10.1)	95 (45.9)	92 (44.4)	20 (9.7)
			NR	276 (47.2)	254 (43.4)	55 (9.4)	201 (46.5)	191 (44.2)	40 (9.3)
rs3755312	*STAT1*	C/G	SR	336 (71.8)	118 (25.2)	14 (3)	142 (68.3)	57 (27.4)	9 (4.3)
			NR	447 (76.7)	127 (21.8)	9 (1.5)	317 (73.5)	107 (24.8)	7 (1.6)
rs2280232	*STAT1*	A/C	SR	337 (72.2)	119 (25.5)	11 (2.4)	157 (75.8)	46 (22.2)	4 (1.9)
			NR	397 (68)	171 (29.3)	16 (2.7)	295 (68.4)	125 (29)	11 (2.6)
rs13029532	*STAT1*	A/C	SR	354 (76.1)	102 (21.9)	9 (1.9)	165 (79.7)	38 (18.4)	4 (1.9)
			NR	426 (72.8)	145 (24.8)	14 (2.4)	322 (74.4)	99 (22.9)	12 (2.8)
rs7562024	*STAT1*	T/C	SR	370 (79.4)	94 (20.2)	2 (0.4)	174 (84.1)	32 (15.5)	1 (0.5)
			NR	459 (78.6)	116 (19.9)	9 (1.5)	349 (81)	76 (17.6)	6 (1.4)
rs1914408	*STAT1*	C/T	SR	218 (46.6)	195 (41.7)	55 (11.8)	86 (41.3)	92 (44.2)	30 (14.4)
			NR	249 (42.6)	264 (45.1)	72 (12.3)	189 (43.8)	191 (44.2)	52 (12)
rs2066807	*STAT2*	C/G	SR	424 (90.6)	43 (9.2)	1 (0.2)	189 (90.9)	18 (8.7)	1 (0.5)
			NR	523 (89.4)	60 (10.3)	2 (0.3)	392 (90.7)	40 (9.3)	0 (0)
rs12432194	IFN regulatory factor 9	C/T	SR	263 (56.4)	172 (36.9)	31 (6.7)	119 (57.5)	77 (37.2)	11 (5.3)
			NR	347 (59.1)	203 (34.6)	37 (6.3)	254 (58.5)	153 (35.3)	27 (6.2)
rs4981494	IFN regulatory factor 9	G/A	SR	202 (43.4)	211 (45.4)	52 (11.2)	95 (45.9)	91 (44)	21 (10.1)
			NR	272 (46.7)	250 (42.9)	61 (10.5)	197 (45.8)	187 (43.5)	46 (10.7)
rs12432304	IFN regulatory factor 9	C/T	SR	130 (27.9)	225 (48.3)	111 (23.8)	61 (29.5)	99 (47.8)	47 (22.7)
			NR	158 (27.2)	282 (48.6)	140 (24.1)	120 (28)	203 (47.4)	105 (24.5)
rs2277484	IFN regulatory factor 9	G/A	SR	337 (72.6)	110 (23.7)	17 (3.7)	154 (74.4)	45 (21.7)	8 (3.9)
			NR	401 (68.4)	170 (29)	15 (2.6)	295 (68)	127 (29.3)	12 (2.8)
rs2236350	IFN regulatory factor 9	C/A	SR	206 (44)	209 (44.7)	53 (11.3)	88 (42.3)	98 (47.1)	22 (10.6)
			NR	254 (43.6)	269 (46.1)	60 (10.3)	189 (43.8)	194 (44.9)	49 (11.3)
rs2303364	Ras-related C3 botulinum toxin substrate 1	C/T	SR	162 (34.8)	229 (49.2)	74 (15.9)	67 (32.5)	102 (49.5)	37 (18)
			NR	196 (33.7)	275 (47.3)	111 (19.1)	137 (31.9)	214 (49.8)	79 (18.4)
rs836483	Ras-related C3 botulinum toxin substrate 1	G/A	SR	384 (82.6)	76 (16.3)	5 (1.1)	171 (82.6)	35 (16.9)	1 (0.5)
			NR	472 (80.7)	110 (18.8)	3 (0.5)	346 (79.9)	84 (19.4)	3 (0.7)
rs6954996	Ras-related C3 botulinum toxin substrate 1	G/A	SR	412 (88.6)	51 (11)	2 (0.4)	182 (88.3)	23 (11.2)	1 (0.5)
			NR	513 (87.8)	68 (11.6)	3 (0.5)	377 (87.3)	52 (12)	3 (0.7)
rs7456834	Ras-related C3 botulinum toxin substrate 1	G/C	SR	307 (66)	144 (31)	14 (3)	133 (64.6)	62 (30.1)	11 (5.3)
			NR	370 (63.5)	197 (33.8)	16 (2.7)	270 (62.5)	151 (35)	11 (2.5)
rs702484	Ras-related C3 botulinum toxin substrate 1	G/C	SR	320 (68.5)	135 (28.9)	12 (2.6)	142 (68.3)	60 (28.8)	6 (2.9)
			NR	393 (67.2)	178 (30.4)	14 (2.4)	285 (66)	135 (31.3)	12 (2.8)
rs2347339	Ras-related C3 botulinum toxin substrate 1	C/G	SR	305 (65.3)	137 (29.3)	25 (5.4)	132 (63.8)	60 (29)	15 (7.2)
			NR	368 (63.1)	182 (31.2)	33 (5.7)	268 (62.2)	141 (32.7)	22 (5.1)
rs768409	Ras-related C3 botulinum toxin substrate 1	A/T	SR	456 (97.9)	10 (2.1)	0 (0)	202 (97.6)	5 (2.4)	0 (0)
			NR	579 (99.1)	5 (0.9)	0 (0)	428 (99.1)	4 (0.9)	0 (0)
rs2305871	*MAPKK3*	G/C	SR	241 (51.6)	202 (43.3)	24 (5.1)	104 (50.2)	89 (43)	14 (6.8)
			NR	317 (54.3)	223 (38.2)	44 (7.5)	233 (53.9)	164 (38)	35 (8.1)
rs9901404	*MAPKK3*	G/A	SR	207 (44.4)	212 (45.5)	47 (10.1)	97 (46.9)	93 (44.9)	17 (8.2)
			NR	232 (39.7)	271 (46.4)	81 (13.9)	180 (41.8)	193 (44.8)	58 (13.5)
rs12602109	*MAPKK3*	G/A	SR	167 (36)	224 (48.3)	73 (15.7)	76 (36.7)	94 (45.4)	37 (17.9)
			NR	238 (41.2)	265 (45.9)	74 (12.8)	174 (40.8)	193 (45.3)	59 (13.8)

Supplementary Table 2. (Continued)

SNP	Gene	Alleles (1/2)	Group	All patients with HCV infection: No. of genotypes (%) 1/1	1/2	2/2	Patients with HCV genotype 1b: No. of genotypes (%) 1/1	1/2	2/2
rs3760201	*MAPKK3*	A/G	SR	198 (42.6)	217 (46.7)	50 (10.8)	98 (47.3)	88 (42.5)	21 (10.1)
			NR	222 (38.5)	275 (47.7)	80 (13.9)	169 (39.4)	199 (46.4)	61 (14.2)
rs8074866	*MAPKK3*	C/T	SR	248 (53.2)	195 (41.8)	23 (4.9)	110 (53.1)	84 (40.6)	13 (6.3)
			NR	343 (58.9)	207 (35.6)	32 (5.5)	257 (59.6)	148 (34.3)	26 (6)
rs2074028	*MAPKK6*	T/C	SR	170 (36.5)	233 (50)	63 (13.5)	65 (31.3)	109 (52.4)	34 (16.3)
			NR	200 (34.2)	283 (48.4)	102 (17.4)	144 (33.3)	211 (48.8)	77 (17.8)
rs2034100	*MAPKK6*	G/A	SR	409 (87.6)	56 (12)	2 (0.4)	181 (87.4)	25 (12.1)	1 (0.5)
			NR	518 (88.7)	64 (11)	2 (0.3)	381 (88.2)	49 (11.3)	2 (0.5)
rs817565	*MAPKK6*	T/G	SR	125 (26.8)	214 (45.9)	127 (27.3)	66 (31.9)	87 (42)	54 (26.1)
			NR	159 (27.1)	284 (48.4)	144 (24.5)	115 (26.5)	216 (49.8)	103 (23.7)
rs2251862	*MAPKK6*	C/A	SR	231 (49.6)	193 (41.4)	42 (9)	88 (42.7)	95 (46.1)	23 (11.2)
			NR	263 (45)	259 (44.3)	62 (10.6)	186 (43)	198 (45.7)	49 (11.3)
rs2072073	*MAPKK6*	C/G	SR	239 (51.3)	183 (39.3)	44 (9.4)	112 (54.1)	76 (36.7)	19 (9.2)
			NR	272 (46.5)	264 (45.1)	49 (8.4)	204 (47.1)	196 (45.3)	33 (7.6)
rs2716213	*MAPKK6*	T/G	SR	159 (34)	222 (47.5)	86 (18.4)	58 (28)	103 (49.8)	46 (22.2)
			NR	201 (34.4)	274 (46.8)	110 (18.8)	140 (32.4)	202 (46.8)	90 (20.8)
rs12451722	*MAPKK6*	T/C	SR	304 (65.2)	145 (31.1)	17 (3.6)	141 (67.8)	56 (26.9)	11 (5.3)
			NR	382 (65.5)	177 (30.4)	24 (4.1)	283 (65.5)	129 (29.9)	20 (4.6)
rs6501326	*MAPKK6*	A/G	SR	187 (40.3)	216 (46.6)	61 (13.1)	76 (36.9)	96 (46.6)	34 (16.5)
			NR	231 (39.5)	268 (45.8)	86 (14.7)	167 (38.6)	204 (47.1)	62 (14.3)
rs2716225	*MAPKK6*	G/A	SR	345 (73.7)	108 (23.1)	15 (3.2)	152 (73.1)	46 (22.1)	10 (4.8)
			NR	437 (74.4)	141 (24)	9 (1.5)	336 (77.4)	93 (21.4)	5 (1.2)
rs8080760	*MAPKK6*	A/G	SR	143 (30.8)	233 (50.2)	88 (19)	62 (30.1)	105 (51)	39 (18.9)
			NR	177 (30.3)	294 (50.3)	114 (19.5)	131 (30.3)	213 (49.3)	88 (20.4)
rs12948059	*MAPKK6*	A/G	SR	341 (73.3)	112 (24.1)	12 (2.6)	160 (77.3)	43 (20.8)	4 (1.9)
			NR	418 (71.7)	153 (26.2)	12 (2.1)	323 (75.1)	100 (23.3)	7 (1.6)
rs2074027	*MAPKK6*	A/G	SR	156 (33.4)	223 (47.8)	88 (18.8)	79 (38)	92 (44.2)	37 (17.8)
			NR	206 (35.2)	264 (45.1)	115 (19.7)	156 (36)	188 (43.4)	89 (20.6)
rs2716222	*MAPKK6*	C/T	SR	186 (39.9)	217 (46.6)	63 (13.5)	86 (41.5)	93 (44.9)	28 (13.5)
			NR	260 (44.4)	244 (41.7)	81 (13.8)	194 (44.8)	180 (41.6)	59 (13.6)
rs4968857	*MAPKK6*	T/C	SR	144 (30.9)	232 (49.8)	90 (19.3)	77 (37.4)	88 (42.7)	41 (19.9)
			NR	192 (32.9)	275 (47.1)	117 (20)	143 (33.2)	205 (47.6)	83 (19.3)
rs756944	*MAPKK6*	T/C	SR	151 (32.5)	229 (49.2)	85 (18.3)	76 (37.1)	87 (42.4)	42 (20.5)
			NR	188 (32.2)	298 (51)	98 (16.8)	143 (33.2)	215 (49.9)	73 (16.9)
rs2715806	*MAPKK6*	G/A	SR	197 (42.5)	209 (45)	58 (12.5)	92 (44.4)	89 (43)	26 (12.6)
			NR	272 (46.5)	243 (41.5)	70 (12)	210 (48.6)	170 (39.4)	52 (12)
rs8078890	*MAPKK6*	A/C	SR	136 (29.2)	225 (48.3)	105 (22.5)	63 (30.4)	93 (44.9)	51 (24.6)
			NR	176 (30.1)	279 (47.8)	129 (22.1)	132 (30.6)	201 (46.6)	98 (22.7)
rs2716191	*MAPKK6*	C/T	SR	341 (73.3)	116 (24.9)	8 (1.7)	149 (72)	54 (26.1)	4 (1.9)
			NR	457 (78.3)	121 (20.7)	6 (1)	336 (77.8)	91 (21.1)	5 (1.2)
rs2715812	*MAPKK6*	C/T	SR	229 (49)	191 (40.9)	47 (10.1)	106 (51)	83 (39.9)	19 (9.1)
			NR	255 (43.6)	266 (45.5)	64 (10.9)	180 (41.7)	199 (46.1)	53 (12.3)
rs11869073	*MAPKK6*	A/C	SR	379 (81)	81 (17.3)	8 (1.7)	170 (81.7)	35 (16.8)	3 (1.4)
			NR	480 (81.8)	104 (17.7)	3 (0.5)	369 (85)	63 (14.5)	2 (0.5)
rs12945375	*MAPKK6*	A/G	SR	386 (82.7)	74 (15.8)	7 (1.5)	173 (83.6)	31 (15)	3 (1.4)
			NR	488 (83.1)	97 (16.5)	2 (0.3)	374 (86.2)	60 (13.8)	0 (0)
rs12939509	*MAPKK6*	A/G	SR	422 (90.2)	44 (9.4)	2 (0.4)	186 (89.4)	21 (10.1)	1 (0.5)
			NR	518 (88.2)	67 (11.4)	2 (0.3)	383 (88.2)	49 (11.3)	2 (0.5)
rs8082399	*MAPKK6*	G/A	SR	382 (81.8)	83 (17.8)	2 (0.4)	166 (79.8)	40 (19.2)	2 (1)
			NR	499 (85.4)	82 (14)	3 (0.5)	371 (86.1)	57 (13.2)	3 (0.7)
rs2716195	*MAPKK6*	G/A	SR	315 (67.7)	141 (30.3)	9 (1.9)	141 (68.4)	61 (29.6)	4 (1.9)
			NR	402 (68.7)	165 (28.2)	18 (3.1)	296 (68.5)	120 (27.8)	16 (3.7)
rs2716223	*MAPKK6*	G/A	SR	129 (27.7)	230 (49.4)	107 (23)	54 (26)	100 (48.1)	54 (26)
			NR	155 (26.5)	279 (47.7)	151 (25.8)	104 (24.1)	209 (48.4)	119 (27.5)
rs2715810	*MAPKK6*	G/A	SR	118 (25.3)	237 (50.7)	112 (24)	51 (24.6)	105 (50.7)	51 (24.6)
			NR	147 (25.1)	287 (49.1)	151 (25.8)	106 (24.5)	210 (48.6)	116 (26.9)
rs7213686	*MAPKK6*	T/C	SR	415 (88.9)	50 (10.7)	2 (0.4)	185 (89.4)	21 (10.1)	1 (0.5)
			NR	516 (87.9)	69 (11.8)	2 (0.3)	381 (87.8)	51 (11.8)	2 (0.5)

Supplementary Table 2. (Continued)

SNP	Gene	Alleles (1/2)	Group	All patients with HCV infection: No. of genotypes (%) 1/1	1/2	2/2	Patients with HCV genotype 1b: No. of genotypes (%) 1/1	1/2	2/2
rs8067307	*MAPKK6*	C/A	SR	310 (66.4)	144 (30.8)	13 (2.8)	134 (64.7)	68 (32.9)	5 (2.4)
			NR	370 (63.1)	197 (33.6)	19 (3.2)	285 (65.7)	135 (31.1)	14 (3.2)
rs4968859	*MAPKK6*	A/C	SR	312 (67)	128 (27.5)	26 (5.6)	136 (65.4)	60 (28.8)	12 (5.8)
			NR	364 (62.2)	194 (33.2)	27 (4.6)	269 (62.3)	140 (32.4)	23 (5.3)
rs9893349	*MAPKK6*	G/A	SR	136 (29.3)	233 (50.2)	95 (20.5)	63 (30.6)	94 (45.6)	49 (23.8)
			NR	154 (26.3)	312 (53.2)	120 (20.5)	116 (26.8)	228 (52.7)	89 (20.6)
rs17690015	*MAPKK6*	G/A	SR	386 (82.7)	78 (16.7)	3 (0.6)	180 (87)	27 (13)	0 (0)
			NR	475 (81.2)	104 (17.8)	6 (1)	362 (83.8)	67 (15.5)	3 (0.7)
rs2715834	*MAPKK6*	G/C	SR	128 (27.4)	239 (51.2)	100 (21.4)	50 (24)	113 (54.3)	45 (21.6)
			NR	148 (25.3)	299 (51)	139 (23.7)	112 (25.9)	217 (50.1)	104 (24)
rs1548444	*MAPKK6*	T/G	SR	216 (46.6)	190 (40.9)	58 (12.5)	100 (48.8)	75 (36.6)	30 (14.6)
			NR	232 (39.8)	286 (49.1)	65 (11.1)	166 (38.6)	210 (48.8)	54 (12.6)
rs2715817	*MAPKK6*	T/C	SR	181 (38.7)	209 (44.7)	78 (16.7)	83 (39.9)	88 (42.3)	37 (17.8)
			NR	226 (38.6)	269 (45.9)	91 (15.5)	170 (39.3)	201 (46.4)	62 (14.3)
rs2715832	*MAPKK6*	T/C	SR	276 (59.2)	162 (34.8)	28 (6)	103 (49.8)	86 (41.5)	18 (8.7)
			NR	312 (53.4)	231 (39.6)	41 (7)	223 (51.7)	179 (41.5)	29 (6.7)
rs7761118	p38 MAP kinase	G/A	SR	398 (85.2)	67 (14.3)	2 (0.4)	175 (84.1)	32 (15.4)	1 (0.5)
			NR	494 (84.6)	86 (14.7)	4 (0.7)	366 (84.7)	64 (14.8)	2 (0.5)
rs2145362	p38 MAP kinase	C/G	SR	142 (30.5)	238 (51.2)	85 (18.3)	57 (27.5)	114 (55.1)	36 (17.4)
			NR	193 (32.9)	281 (48)	112 (19.1)	143 (33)	205 (47.3)	85 (19.6)
rs3752525	p38 MAP kinase	G/T	SR	254 (54.3)	192 (41)	22 (4.7)	107 (51.4)	89 (42.8)	12 (5.8)
			NR	319 (54.3)	226 (38.5)	42 (7.2)	233 (53.7)	169 (38.9)	32 (7.4)
rs3730326	p38 MAP kinase	G/T	SR	433 (92.5)	31 (6.6)	4 (0.9)	191 (91.8)	15 (7.2)	2 (1)
			NR	543 (92.7)	42 (7.2)	1 (0.2)	403 (93.1)	30 (6.9)	0 (0)
rs7770710	p38 MAP kinase	C/T	SR	418 (89.5)	49 (10.5)	0 (0)	190 (91.3)	18 (8.7)	0 (0)
			NR	544 (92.8)	40 (6.8)	2 (0.3)	398 (91.9)	35 (8.1)	0 (0)
rs16884694	p38 MAP kinase	G/A	SR	354 (76)	107 (23)	5 (1.1)	161 (77.4)	46 (22.1)	1 (0.5)
			NR	453 (77.8)	120 (20.6)	9 (1.5)	334 (77.7)	91 (21.2)	5 (1.2)
rs13196204	p38 MAP kinase	T/G	SR	293 (63)	164 (35.3)	8 (1.7)	122 (58.9)	81 (39.1)	4 (1.9)
			NR	387 (66.6)	170 (29.3)	24 (4.1)	282 (65.4)	132 (30.6)	17 (3.9)
rs3804453	p38 MAP kinase	A/G	SR	401 (85.9)	65 (13.9)	1 (0.2)	181 (87)	27 (13)	0 (0)
			NR	508 (86.8)	71 (12.1)	6 (1)	369 (85.4)	60 (13.9)	3 (0.7)
rs3804454	p38 MAP kinase	T/G	SR	364 (77.9)	93 (19.9)	10 (2.1)	162 (77.9)	39 (18.8)	7 (3.4)
			NR	451 (77.2)	124 (21.2)	9 (1.5)	338 (78.2)	89 (20.6)	5 (1.2)
rs10807156	p38 MAP kinase	A/T	SR	164 (35)	235 (50.2)	69 (14.7)	66 (31.7)	115 (55.3)	27 (13)
			NR	217 (37.3)	271 (46.6)	94 (16.2)	159 (36.7)	202 (46.7)	72 (16.6)
rs4844550	*MAPKAPK2*	A/G	SR	228 (49.1)	195 (42)	41 (8.8)	103 (49.5)	85 (40.9)	20 (9.6)
			NR	292 (50)	241 (41.3)	51 (8.7)	211 (49)	174 (40.4)	46 (10.7)
rs10863784	*MAPKAPK2*	C/G	SR	135 (29.2)	224 (48.4)	104 (22.5)	62 (30.4)	96 (47.1)	46 (22.5)
			NR	161 (27.4)	293 (49.9)	133 (22.7)	113 (26)	217 (50)	104 (24)
rs12028997	*MAPKAPK2*	C/T	SR	400 (85.5)	66 (14.1)	2 (0.4)	177 (85.1)	31 (14.9)	0 (0)
			NR	501 (85.5)	80 (13.7)	5 (0.9)	374 (86.4)	55 (12.7)	4 (0.9)
rs4073250	*MAPKAPK2*	C/T	SR	394 (84.9)	68 (14.7)	2 (0.4)	181 (87.9)	25 (12.1)	0 (0)
			NR	492 (84.4)	87 (14.9)	4 (0.7)	360 (83.7)	66 (15.3)	4 (0.9)
rs4072677	*MAPKAPK2*	T/G	SR	186 (39.9)	218 (46.8)	62 (13.3)	83 (40.1)	94 (45.4)	30 (14.5)
			NR	224 (38.2)	288 (49.1)	75 (12.8)	162 (37.3)	211 (48.6)	61 (14.1)
rs12060808	*MAPKAPK2*	C/T	SR	382 (81.8)	77 (16.5)	8 (1.7)	175 (84.5)	28 (13.5)	4 (1.9)
			NR	473 (81)	103 (17.6)	8 (1.4)	347 (80.5)	78 (18.1)	6 (1.4)
rs616589	*MAPKAPK3*	G/A	SR	215 (46)	205 (43.9)	47 (10.1)	111 (53.4)	84 (40.4)	13 (6.3)
			NR	235 (40.3)	271 (46.5)	77 (13.2)	164 (38)	209 (48.4)	59 (13.7)
rs3792323	*MAPKAPK3*	A/T	SR	242 (51.8)	187 (40)	38 (8.1)	124 (59.6)	75 (36.1)	9 (4.3)
			NR	273 (46.7)	253 (43.3)	58 (9.9)	189 (43.9)	196 (45.5)	46 (10.7)
rs3804628	*MAPKAPK3*	G/A	SR	416 (89.3)	48 (10.3)	2 (0.4)	184 (88.5)	22 (10.6)	2 (1)
			NR	519 (88.4)	66 (11.2)	2 (0.3)	389 (89.6)	43 (9.9)	2 (0.5)
rs2040397	*MAPKAPK3*	C/T	SR	288 (61.8)	155 (33.3)	23 (4.9)	124 (59.9)	74 (35.7)	9 (4.3)
			NR	393 (67)	170 (29)	24 (4.1)	282 (65)	132 (30.4)	20 (4.6)

NOTE. Genotype data are presented as the number of subjects with percentages in parentheses. Allele 1, major allele; Allele 2, minor allele.

HUMAN GENE THERAPY 21:40–50 (January 2010)

DOI: 10.1089/hum.2009.027

In Vivo Stable Transduction of Humanized Liver Tissue in Chimeric Mice via High-Capacity Adenovirus–Lentivirus Hybrid Vector

Shuji Kubo,[1,2] Miho Kataoka,[3] Chise Tateno,[3] Katsutoshi Yoshizato,[3,4] Yoshiko Kawasaki,[2] Takahiro Kimura,[1] Emmanuelle Faure-Kumar,[1] Donna J. Palmer,[5] Philip Ng,[5] Haruki Okamura,[2] and Noriyuki Kasahara[1]

Abstract

We developed hybrid vectors employing high-capacity adenovirus as a first-stage carrier encoding all the components required for *in situ* production of a second-stage lentivirus, thereby achieving stable transgene expression in secondary target cells. Such vectors have never previously been tested in normal tissues, because of the scarcity of suitable *in vivo* systems permissive for second-stage lentivirus assembly. Here we employed a novel murine model in which endogenous liver tissue is extensively reconstituted with engrafted human hepatocytes, and successfully achieved stable transduction by the second-stage lentivirus produced *in situ* from first-stage adenovirus. This represents the first demonstration of the functionality of adenoviral-lentiviral hybrid vectors in a normal parenchymal organ *in vivo*.

Introduction

ADENOVIRAL VECTORS (AdVs) have been successfully used *in vivo* to transduce various postmitotic tissues, but generally only transient gene expression can be achieved because of cytotoxic T-lymphocyte–mediated immune responses against viral genes retained in conventional AdVs, and their extremely low frequency of chromosomal integration (Harui *et al.*, 1999; Wivel *et al.*, 1999). More persistent expression can be maintained by high-capacity, helper-dependent AdVs (HDAdVs) from which all of the viral coding sequences have been removed (Parks *et al.*, 1996; Schiedner *et al.*, 1998; Kochanek, 1999; Kim *et al.*, 2001; Oka *et al.*, 2001), but its duration is still limited because of progressive dilution of the extrachromosomal HDAdV vector DNA as transduced cells divide. Treatment of hereditary diseases may require more stable, long-term transgene expression, which can be achieved only through permanent integration or ongoing episomal replication of vector DNA.

To overcome this limitation, various hybrid vector systems have been developed, which employ AdV as a first-stage delivery vehicle to efficiently enter target cells, but then utilize the machinery of integrating viruses or mobile genetic elements to achieve permanent chromosomal integration (Feng *et al.*, 1997; Caplen *et al.*, 1999; Lieber *et al.*, 1999; Recchia *et al.*, 1999; Tan *et al.*, 1999; Leblois *et al.*, 2000; Soifer *et al.*, 2001; Soifer *et al.*, 2002; Yant *et al.*, 2002; Kubo and Mitani, 2003; Dorigo *et al.*, 2004; Picard-Maureau *et al.*, 2004). Efficient two-stage transduction *in vitro* and stable long-term transgene expression have previously been demonstrated with AdV–transposon (Soifer *et al.*, 2001; Yant *et al.*, 2002), AdV–adeno-associated virus (Lieber *et al.*, 1999; Recchia *et al.*, 1999), AdV–retrovirus (Feng *et al.*, 1997; Caplen *et al.*, 1999; Soifer *et al.*, 2002), AdV–foamy virus (Picard-Maureau *et al.*, 2004), and AdV–lentivirus (Kubo and Mitani, 2003) vectors. In particular, Kubo and Mitani (2003) have demonstrated the ability of an AdV–lentivirus hybrid vector to efficiently enter a variety of cell types via the first-stage HDAdV and subsequently mediate *in situ* production of a human immunodeficiency virus (HIV)-derived second-stage lentiviral vector (LV), which then stably delivers a marker gene to neighboring cells. However, this hybrid vector generated second-stage LV pseudotyped with the vesicular stomatitis virus G glycoprotein (VSV-G), a highly fusogenic and toxic envelope

[1]Division of Digestive Diseases, Department of Medicine, University of California at Los Angeles, Los Angeles, CA 90095.
[2]Laboratory of Host Defenses, Institute for Advanced Medical Sciences, Hyogo College of Medicine, Nishinomiya, Hyogo 663-8501, Japan.
[3]Yoshizato Project, CLUSTER, Hiroshima Prefectural Institute of Industrial Science and Technology, Higashi-Hiroshima, Hiroshima 739-0046, Japan.
[4]Developmental Biology Laboratory and Hiroshima University 21st Century COE Program for Advanced Radiation Casualty Medicine, Department of Biological Science, Graduate School of Science, Higashi-Hiroshima, Hiroshima 739-8526, Japan.
[5]Center for Cell & Gene Therapy, Baylor College of Medicine, Houston, TX 77030.

protein (Ory *et al.*, 1996), which may result in unwanted cytotoxic effects in the primary target cells during LV production. Further, the ability of AdV-lentivirus hybrid vectors to stably transduce normal quiescent tissues *in vivo* has never previously been tested.

We have now developed an improved high-capacity AdV-lentivirus hybrid vector system, designated HL, and examined the ability of this new hybrid system to mediate efficient and stable gene transfer *in vitro* and *in vivo*. The first-stage HDAdV of the HL hybrid system directs the production of a minimal second-stage LV that retains less than 800 bp of HIV sequence (Chen *et al.*, 2002) and is pseudotyped with the murine leukemia virus (MLV) 4070A amphotropic envelope, which is much less cytotoxic than VSV-G. However, to test the transduction efficiency of the new HL hybrid vector system, target cells that can support *in situ* production of the HIV-derived second-stage LV are required. For *in vitro* experiments, human cell lines permissive for HIV replication can be employed. However, the requirement for human target cells presents a challenge to testing the functionality of the HL hybrid vector system *in vivo*, particularly with respect to its ability to stably transduce normal organs and tissues.

As nearly 90% of the input dose of AdV introduced *in vivo* accumulates in the liver upon intravenous injection (Kass-Eisler *et al.*, 1994; Huard *et al.*, 1995; Kubo *et al.*, 1997), and nearly 100% transduction of hepatocytes can be achieved at higher doses (Li *et al.*, 1993), the liver is an attractive target for *in vivo* testing of the HL system. However, multiple blocks to HIV replication have been reported in rodent cells, including cellular entry, reduced abundance of unspliced HIV-RNA and *gag* proteins, and defects in infectious particle assembly (Hofmann *et al.*, 1999; Bieniasz and Cullen, 2000; Mariani *et al.*, 2000). Therefore, to test the HL hybrid vector *in vivo*, we sought a humanized liver model that is permissive for HIV particle assembly.

Successful reconstitution of human liver tissue has recently been achieved in immunodeficient mice (Dandri *et al.*, 2001; Mercer *et al.*, 2001). Dandri *et al.* (2001) reported that cross-breeding of recombinant activation gene-2–deleted mice with transgenic mice expressing the hepatotoxic urokinase-type plasminogen activator (uPA) results in immunodeficient progeny which undergo progressive liver degeneration. These progeny were successfully transplanted with human hepatocytes, resulting in chimeric liver tissue with a replacement index of up to 15%, rendering these mice permissive for HBV infection (Dandri *et al.*, 2001). Similarly, Mercer *et al.* (2001) demonstrated that uPA/SCID mice bearing chimeric humanized livers with replacement index values of 50% could support HCV replication (Dandri *et al.*, 2001). More extensive repopulation has been difficult to achieve, likely because engrafted human hepatocytes produce complement factors, which appear to exert lethal effects in mice with higher replacement values. However, Tateno *et al.* (2004) and Yoshizato and colleagues (2004) have recently demonstrated that administration of a C5/C3 convertase inhibitor successfully rescued uPA/SCID mice whose chimeric livers proved to be almost completely repopulated with human hepatocytes exhibiting normal cytoarchitecture. The transduction efficiency of oncoretroviral vectors has previously been tested in this humanized liver model, and consistent with their inability to enter quiescent postmitotic cells, was found to be in the order of 5% (Emoto *et al.*, 2005). We have now utilized this unique chimeric liver model to test the ability of the HL hybrid system to mediate efficient entry by the first-stage HDAdV, *in situ* production of the second-stage LV, and stable transduction in fully humanized livers *in vivo*. To our knowledge, this represents the first report of *in vivo* testing of an AdV–lentivirus hybrid vector system in a normal parenchymal organ.

Materials and Methods

Cells

Cell lines including 293 (Graham *et al.*, 1977) (Microbix, Toronto, Canada), 293T (DuBridge *et al.*, 1987), and the Gli36 human glioma (Sena-Esteves *et al.*, 2000) were cultured in Dulbecco's modified Eagle's medium supplemented with 10% fetal calf serum (FCS; Omega, Tarzana, CA). Hep3B human hepatocellular carcinoma cells were cultured in Eagle's minimum essential medium supplemented with 10% FCS, 1 m*M* sodium pyruvate, and nonessential amino acids. Primary human hepatocytes and their specific medium were purchased from Cambrex (Baltimore, MD; CC-2591).

HL first-stage HDAdV construction and production

The phosphoglycerokinase promoter-driven green fluorescence protein (GFP) marker gene cassette, cytomegalovirus promoter (CMV)-driven *gag/pol/rev* lentiviral packaging cassette, simian virus 40 early promoter-driven MLV 4070A amphotropic envelope cassette, and minimal LV construct (Robbins *et al.*, 1998; Chen *et al.*, 2002) were sequentially cloned into the HDAdV plasmid pSTK120, which contains the human Ad5 inverted terminal repeat sequences and packaging signal, resulting in the construction of the complete HL vector plasmid, pHL. Additional details regarding the pHL construct, and the HIV-based minimal LV contained therein, are provided upon request.

The HL vector and control HDAdV cmv-GFP (Ad GFP) were prepared using the FLPe/*FRT* helper virus system (Umana *et al.*, 2001). The vectors were titrated on 293 cells for GFP expression, using a FACScalibur flow cytometer (Becton Dickinson, San Jose, CA), on day 2 post-infection, defined as transducing units per ml (TU/ml). Another control HDAdV, HDΔ28E4LacZ, was prepared as previously described (Palmer and Ng, 2003). Helper virus contamination levels were determined by Southern blot, as previously described (Kubo and Mitani, 2003).

Second-stage LV production after infection with HL first-stage HDAdV

To confirm production of LV in cells (Gli36, HeLa, Hep3B, HepG2 and human primary hepatocytes) infected by the HL vector, 4×10^5 cells of each were infected with various amounts of HL vector. The amount of vector used for each infection was based on the titer determined using each cell line. At 4 hr postinfection, the infected cells were washed three times with phosphate-buffered saline (PBS), and incubated in growth medium. At 48 hr postinfection, the virus-containing medium was harvested, centrifuged, filtered through a 0.45-μm pore filter, and used for titration on 293 cells by X-galactosidase (gal) staining to detect βgal expression. In preliminary experiments, the level of residual adenovirus carried over in the filtered supernatant medium after infection of primary cells at a multiplicity of infection (MOI) of 10, as

measured by flow cytometry for GFP expression in secondary cells, was less than 1%.

To inhibit lentiviral infection, 293 cells were infected with the viral supernatant in the presence or absence of 5 μM zidovudine (AZT; Sigma, St. Louis, MO).

To investigate the kinetics of LV vector production after HL vector infection, 4×10^5 Hep3B cells were infected with HL at various MOIs in six-well plates. The medium was collected at different time points and titrated on 293 cells, as described earlier.

Long-term culture experiments

Hep3B cells (2×10^5) were infected with the HL vector, at an MOI of 10, and incubated in the presence of AZT on a 10-cm dish. The cells were split at a ratio of 1:20 once a week, and expression of GFP was examined by flow cytometry. At each passage, DNA was extracted from a portion of the cells and analyzed for proviral integration by Southern hybridization. A part of the HL-infected cells were also plated on Lab-Tek chamber slides (Thermo Fisher Scientific, Rochester, NY). The next day, the cells were fixed for 10 min with 4% paraformaldehyde, washed with PBS, and incubated with 50 mM NH_4Cl in PBS for 5 min. The cells were permeabilized in 0.5% Triton/PBS for 5 min and then incubated for 30 min in 1% bovine serum albumin/PBS for blocking. The cells were incubated for 1 hr with a 1:1000 dilution of mouse anti-GFP monoclonal (Chemicon, Temecula, CA). Immunoreactivity for GFP was visualized with a 1:5000 dilution of goat anti-mouse immunoglobulin G (IgG) (H + L) Alexa Fluor 488. The cells were then incubated with a 1:1000 dilution of rabbit anti-βgal polyclonal (ab616; Abcam, Cambridge, MA). Immunoreactivities for βgal were visualized with a 1:5000 dilution of goat anti-rabbit IgG (H + L) Alexa Fluor 594 (Molecular Probes, Eugene, OR).

Animals

Chimeric mice with human liver were generated as previously described (Tateno *et al.*, 2004). Briefly, uPA/SCID mice were generated by crossing uPA mice [B6SJL-TgN(Alb1Plau)144Bri; The Jackson Laboratory, Bar Harbor, ME] with SCID mice (Fox Chase SCID C.B-17/Icr-*scid* Jcl; Clea Japan, Tokyo, Japan). The $uPA^{+/+}SCID^{+/+}$ mice were screened by polymerase chain reaction (PCR) and injected with $5.0–7.5\times10^5$ viable human hepatocytes (IVT079; In Vitro Technologies Inc., Baltimore, MD) through a small left-flank incision into the inferior splenic pole at 20–30 days after birth. The mice were injected intraperitoneally with 200 μl of 1.5 mg/ml Futhan (nafamostat mesilate, 6-amidino-2-naphthyl *p*-guanidinobenzoate dimethanesulfonate; gift from Torii Pharmaceutical, Tokyo, Japan) to enhance repopulation of the liver with human hepatocytes. The replacement index was estimated by serum level of human albumin as previously described (Tateno *et al.*, 2004). Generally, >5 mg/ml human albumin in the blood indicates high replacement index values of >70%, and mice screened in this manner were used for experiments at 6–8 weeks posttransplantation.

After injection with gadolinium (10 mg/kg body weight) to eliminate Kupffer cells (Lieber *et al.*, 1997), either HL vector (2×10^9 TU/200 ml) or buffer (PBS) was injected via tail vein, followed by sacrifice at 4 days or 4 weeks postinfection ($n = 4$ per group). A portion of each liver sample was immediately digested into cell suspensions and used for flow cytometric analysis. The remaining portion was frozen in liquid nitrogen for isolation of genomic DNA or for frozen tissue sections. Immunofluorescence (IF) and immunohistochemistry (IHC) for GFP were performed on frozen liver sections using standard methods with GFP-specific antibodies (ab290; Abcam): goat anti-rabbit IgG-Alexa Fluor 488 for IF, or Vectastain ABC kit (Vector Laboratories, Burlingame, CA) and diaminobenzidine for IHC. IF for βgal was also performed using rabbit anti-βgal antibodies (ab616; Abcam) and goat anti-rabbit IgG-Alexa Fluor 594, as earlier. X-gal staining using standard methods was also performed on glutaraldehyde-fixed liver sections, and the proportion of βgal-positive cells was determined by image analysis using the SPOT digital imaging system and NIH ImageJ software (version 1.34). The replacement index of the mouse liver with human hepatocytes was also determined by IHC for human-specific cytokeratin-8 and -18 (CK8/18) as previously described (Tateno *et al.*, 2004) and is defined as the ratio of area occupied by human hepatocytes to the entire area examined. To assess any potential hepatotoxicity, sera were collected from mice at the time of scheduled sacrifice, that is, at 4 weeks after injection with HL vector or PBS, and serum levels of aspartate amino transferase (AST) were measured by automated colorimetric assay.

Molecular analysis of integrated LVs in the liver

High-molecular-weight genomic DNA was extracted from livers injected with HL vector or PBS. For detection of the stably integrated form of the second-stage LV after production from the first-stage HDAdV, high-molecular-weight genomic DNA (500 ng) was subjected to nested PCR to amplify lentiviral integration events close to or within *Alu* repeat sequences in the human genome (Nguyen *et al.*, 2002; Serafini *et al.*, 2004). Briefly, the first PCR (PCR1) was carried out using a sense oligomer specific for the conserved sequences of human *Alu* (*Alu*-s; 5′-TCCCAGCTACTCGGGA GGCTGAGG-3′) and an antisense oligomer specific for the PBS region of HIV-1 upstream of *gag* (5NC2-as; 5′-GAGTC CTGCGTCGAGAGAG-3′). All amplifications were done using 100 μl of reaction mixture containing 200 ng of genomic DNA, 0.4 mM of each dNTP, 0.8 μM of each sense and antisense primer, 5% dimethyl sulfoxide, and 2 U *Taq* DNA polymerase. After the first DNA denaturation at 95°C for 5 min, 30 amplification cycles were performed consisting of denaturation for 1 min at 94°C, annealing for 1 min at 60°C, and extension for 3 min at 72°C. One aliquot (1:100 dilution) of the first PCR products was subjected to a second PCR (PCR2) amplification using the nested primers, LTR9-s (5′-GCCTCAATAAAGCTTGCCTTG-3′) and U5PBS-as (spanning the U5LTR/PBS boundary region) (5′-GGCGCCAC TGCTAGAGATTTT-3′), which amplified a fragment of 121 bp. The nested PCR conditions were similar to those of the first amplification, except for an annealing temperature of 55°C and an extension time of 1 min. Twenty amplification cycles were performed. In control reactions, genomic DNA that had not been subjected to the first round of PCR was also amplified using the second PCR primers to exclude the presence of residual nonintegrated vector DNA. As a loading control, the same DNA samples were subjected to a PCR that amplified a 610-bp region of human β-actin (5′-GATCAT GTTTGAGACCTTCA-3′ and the reverse sequence 5′-ACC

TTGATCTTCATGGTGC-3′), with the following amplification conditions: 95°C for 2 min, then 30 cycles of 95°C for 30 sec, 65°C for 30 sec, and 72°C for 1 min, followed by a final extension at 72°C for 5 min. Amplification products were resolved on 1.5% agarose gel containing ethidium bromide and detected by ultraviolet transillumination.

The copy number of the integrated form of the lentiviral construct in each cell was determined by quantitative real-time PCR (Q-PCR) with βgal-specific primers and probe, designed using Primer Express software V. 1.0 (Applied Biosystems, Foster City, CA). Primer and probe sequences spanned a 91-bp region in the βgal-coding region, consisting of the following sequences: forward primer, 5′-CTATCCC GACCGCCTTACTG-3′; reverse primer, 5′-GTTTTCGCTCG GGAAGACGTA-3′; probe, 5′-FAM-CAGCGGTCAAAA CAG-TAMRA-3′. Amplification was performed in a reaction volume of 25 μl under the following conditions: 300 ng of high-molecular-weight genomic DNA, 1×Taqman universal PCR master mix (Applied Biosystems), 600 n*M* forward primer, 900 n*M* reverse primer, and 100 n*M* probe. Thermal cycling conditions were 2 min incubation at 50°C, 10 min at 95°C, followed by 40 cycles of successive incubation at 95°C for 15 sec and 60°C for 1 min. Standard curves were generated using serial dilutions of HL vector plasmid, pHL, from 5 to 50,000,000 copies in a background of 50,000 equivalents (300 ng) of untransduced genomic DNA from the chimeric mouse liver. Duplicate samples were amplified in an ABI Prism 7700 sequence detector with continuous fluorescence monitoring. Data were collected and analyzed using 7700 Sequence Detection System software v.1.6.3. (Applied Biosystems). The copy number per cell of integrated lentiviral construct was calculated as the average copy number divided by 50,000 cells (equivalent to 300 ng genomic DNA).

Statistical analysis

The results are presented as mean ± standard deviation. Statistical significance of differences was calculated using Student's *t*-test, and a *p*-value of <0.01 was considered significant.

Results

Design and production of the HL hybrid vector

The hybrid vector HL contains a complete set of HIV-derived lentiviral packaging components incorporated into an HDAdV (Fig. 1A), including (1) a multiple attenuated packaging construct expressing *gag-pol*, *rev*, and the *rev* response element sequence, (2) an envelope construct expressing amphotropic (i.e., broad mammalian host range) *env* from MLV strain 4070A, and (3) a minimal HIV-based LV transfer vector encoding a βgal marker gene driven by a methylation-resistant MLV promoter (MND promoter) (Chen *et al.*, 2002). As this transfer vector sequence contains a LV packaging signal so that its mRNA will be encapsidated by the coexpressed packaging and envelope components to form LV virions, the βgal transgene will not only be expressed in cells directly infected by the HDAdV, but also be transmitted to adjacent cells. The adenoviral backbone

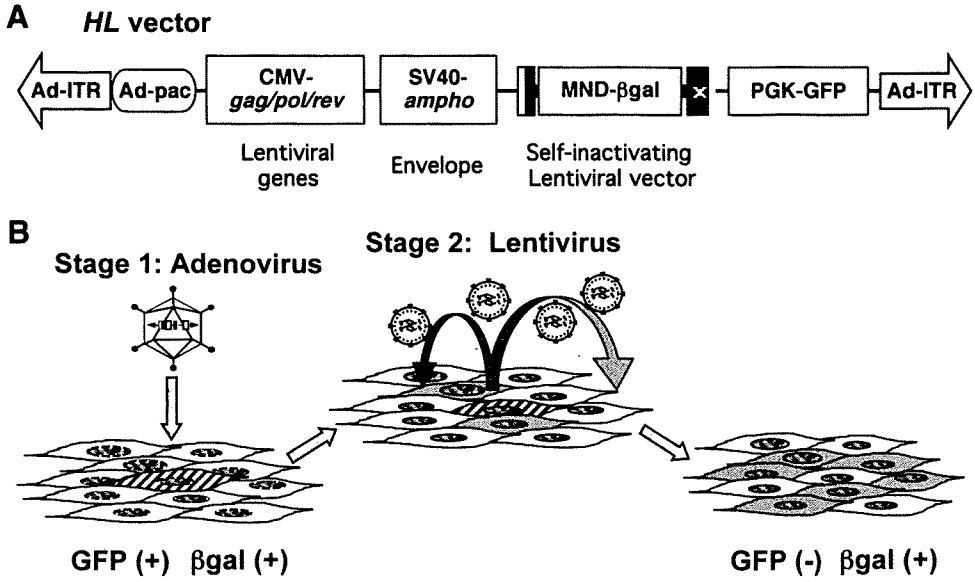

FIG. 1. Outline of the high-capacity adenovirus/lentivirus hybrid vector (HL vector) system. (**A**) Schematic structure of the HL vector. An HL vector is a helper-dependent adenoviral vector encoding expression cassettes for production of a lentiviral vector (LV) based on human immunodeficiency virus 1 (HIV-1). The HL vector has two inverted terminal repeats (Ad-ITR) and the packaging signal (Ad-pac) of human adenovirus type 5 and encodes four gene expression cassettes: (1) a self-inactivating minimal LV that contains the central polypurine tract, the woodchuck hepatitis virus posttranscriptional regulatory element, and the β-galactosidase gene (βgal) driven by the methylation-resistant murine leukemia virus LTR promoter (MND) (Robbins *et al.*, 1998; Chen *et al.*, 2002) as a marker; (2) HIV-*gag/pol/rev* coding sequences driven by cytomegalovirus (CMV) promoter; (3) the amphotropic murine leukemia virus envelope driven by the simian virus 40 early promoter (SV40) for pseudotyping of the lentivirus; and (4) the enhanced green fluorescent protein (GFP) driven by phosphoglycerokinase (PGK) promoter as a marker of the adenoviral backbone. (**B**) Two-stage transduction with the HL vector. The HL vector infects the initial target cells efficiently as an adenoviral vector and produces an LV *in situ*. The LV then infects surrounding secondary target cells and integrates into chromosomes for stable gene expression.

sequence also contains a GFP expression cassette unlinked to the LV components; the GFP marker gene will not be encapsidated into LV particles, thereby allowing specific quantitation of initial transduction by HDAdV itself. Thus, it is possible to distinguish between untransduced cells [GFP (−), βgal(−)], cells transduced by HL first-stage HDAdV only [GFP(+), βgal(+)], and cells transduced by HL second-stage LV [GFP(−), βgal(+)] (Fig. 1B).

The first-stage HDAdV was propagated using the FRT/FLPe helper system (Umana *et al.*, 2001). The GFP titers of purified HL vector preparations on 293 cells ranged from 4.1×10^9 to 1.8×10^{10} TU/ml. Vector stocks contained less than 0.1% helper virus contamination, as determined by Southern hybridization, using a probe for the adenoviral packaging signal (data not shown).

Infection with HL first-stage HDAdV results in production of functional second-stage LV

Following infection by the HL first-stage HDAdV vector at various MOIs, cell-free conditioned media from various human cell lines, including Gli36 (glioma), HeLa (cervical adenocarcinoma), and Hep3B and HepG2 (both hepatocellular carcinoma), were inoculated into fresh 293 cell cultures and tested for their ability to mediate secondary transmission of βgal expression. For all primary target cell lines tested, increasing MOI during first-stage HDAdV transduction correlated with increasing βgal transmission to secondary target cells (Fig. 2A). Further, βgal expression in secondary target cells was markedly suppressed by the reverse transcriptase inhibitor AZT, indicating that the observed transmission was indeed mediated by second-stage LV and was not due to carry-over of the first-stage HDAdV or pseudotransduction by overexpressed βgal protein (Fig. 2B). Of the cell lines tested, Gli36 and Hep3B produced the highest titers of LV (1.0×10^4 and 5.1×10^4 TU/ml, respectively, at MOI = 100) (Fig. 2A), which also correlated with high levels of p24 production (236 and 316 ng/ml, respectively). Primary human hepatocytes also produced LV at titers of 6.0×10^1, 1.0×10^3, and 1.2×10^4 TU/ml upon infection with 1, 10, and 100 μl of HL vector (4.0×10^8 TU/ml), respectively. Taken together, these findings indicate that the HL hybrid vector is

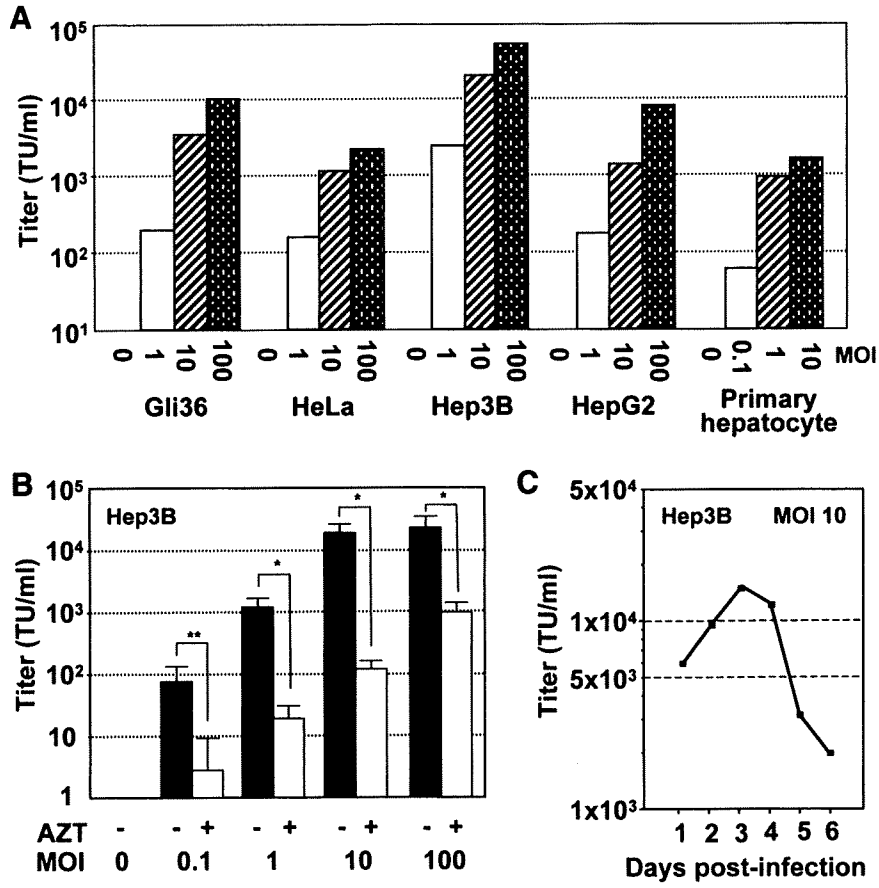

FIG. 2. Production of LV via HL vector system. (A) Production of LV in a variety of cell types after HL infection. Various cell lines indicated in the figure were infected with HL at multiplicity of infections (MOIs) of 1, 10, or 100. After 48 hr, viral supernatant was collected and titrated on 293 cells for βgal expression. (B) Production of LV following HL vector infection. Hep3B cells were infected with the HL vector at MOIs of 0.1, 1, 10, or 100. After 48 hr, viral supernatant was collected and titrated on 293 cells for βgal expression in the presence or absence of zidovudine (AZT, 5 μM). Data shown are average titers and standard deviations from the experiment performed in triplicate. Effect of AZT on titers was determined by Student's *t*-test (**$p < 0.05$, *$p < 0.01$). (C) Time course of lentiviral production from Hep3B cells infected with the HL vector. Hep3B cells were infected with HL at an MOI of 10 and monitored for up to 6 days. At different time points indicated in the figure, the medium was replaced, and the viral supernatant was titrated for βgal expression on 293 cells.

capable of directing the production of infectious LV particles from a variety of cell types, and that the LV yield is dependent upon the MOI and the target cell type.

To determine how long cells can produce LV after being infected with the HL first-stage HDAdV vector, a time-course experiment was performed. After infection of Hep3B cells with the HL first-stage HDAdV vector at an MOI of 10, the culture medium was harvested and replaced with fresh medium every day. The LV titers of the conditioned media harvested daily were measured on secondary target cells and were found to increase, reaching a peak level by day 3 post-HDAdV infection (1.3×10^4 TU/ml; Fig. 2C). Thereafter, HL-infected human cells continued to sustain LV production for several days (postinfection day 6 titer = 2.0×10^3 TU/ml).

In vitro *persistence of second-stage LV-transduced cells following HL first-stage HDAdV infection*

The spread of lentivirus in long-term cultures of HL-infected cells was examined by maintaining infected Hep3B in culture (Fig. 3A). As expected, GFP expression from the adenovirus backbone significantly decreased over time because of ongoing cell division-mediated dilution of HDAdV episomes in the culture. The percentage of GFP-positive cells

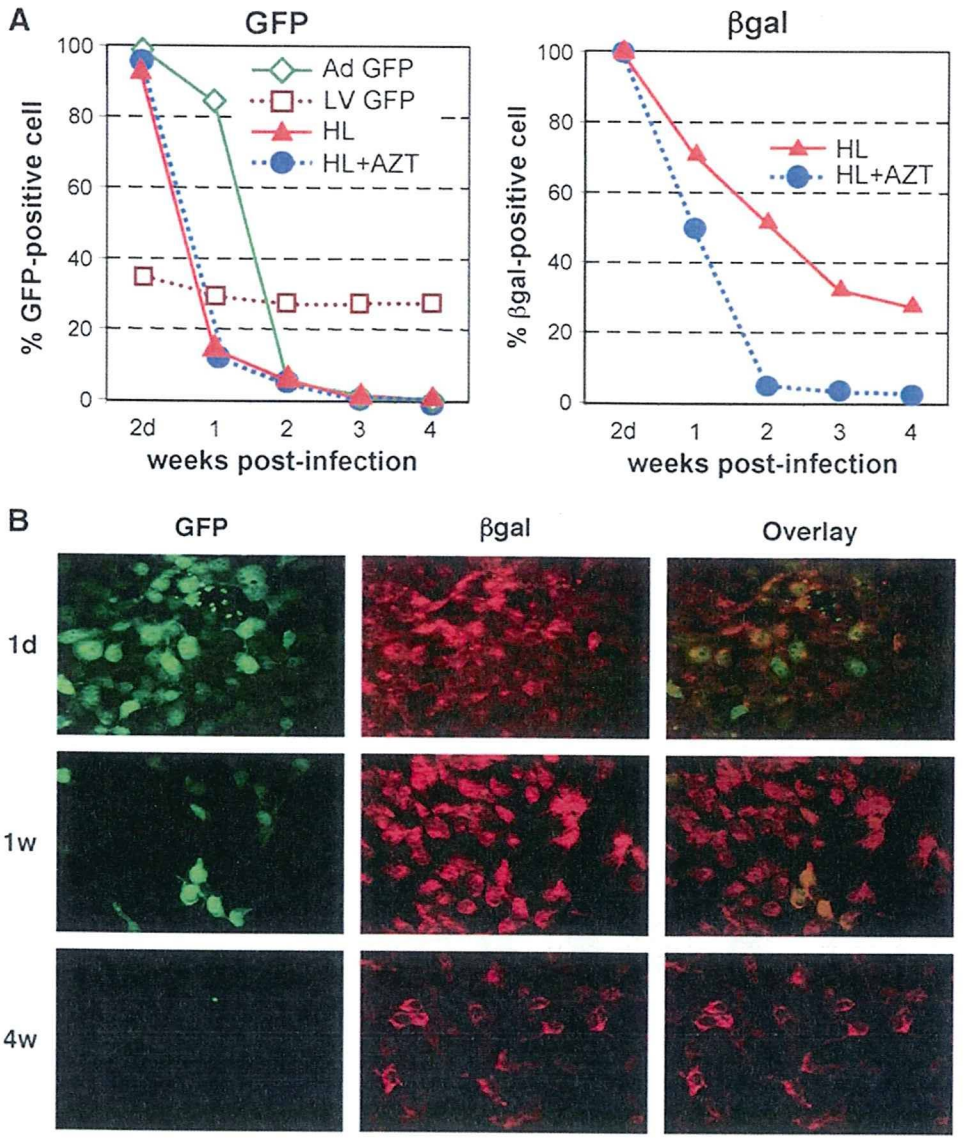

FIG. 3. Spread of LV-transduced cells and persistent gene expression following HL vector infection. (**A**) Transduction efficiencies of HL hybrid vector-infected cells. Hep3B cells (2×10^5) infected with the HL vector at an MOI of 10 were incubated overnight, and the cells were split the following day and cultivated in the presence (blue circle) or absence (red triangle) of AZT on a 10-cm dish. The control samples infected with an LV GFP (brown square) or an Ad GFP (green diamond) are also shown. The cells were passaged at a ratio of 1:20 every week, and expressions of GFP and βgal were examined. Data are representative of three independent experiments, all yielding similar results. (**B**) Persistent gene expression achieved via HL hybrid vector system in transformed human hepatocytes *in vitro*. Hep3B cells were infected with HL vector at an MOI of 10. The cells were passaged at a ratio of 1:20 every week. Expressions of GFP and βgal were analyzed by immunofluorescence staining using anti-GFP and anti-βgal antibody at the indicated time points after HL infection.

quickly decreased from > 90% to <2% within 2 weeks postinfection in the HL-infected cells (HL and HL + AZT) as well as in cells infected with control Ad GFP. Initially, a parallel decrease in βgal-positive cells was observed. However, 25% of the HL-infected cells (HL) remained βgal positive at 4 weeks postinfection, whereas those in the HL-infected/AZT-treated cells (HL + AZT) were <2% βgal positive within 2 weeks postinfection. Persistent βgal expression in the HL-infected cells (HL) was also confirmed by IF staining (Fig. 3B). Southern hybridization of high-molecular-weight genomic DNA extracted from the cells at week 4 confirmed LV proviral integration and a direct correlation between βgal expression and the copy number of the integrated βgal transgenes (data not shown). This also demonstrates that persistent βgal expression in the HL-infected cells is mediated by stable transduction with the HL second-stage LV vector.

In vivo *persistence of second-stage LV-transduced cells in humanized liver following intravenous administration of HL first-stage HDAdV*

In vivo testing of the HL vector system requires a model that is permissive for assembly of human lentivirus. We employed a unique humanized model in which endogenous murine hepatocytes are extensively replaced with human hepatocytes. The replacement indices, calculated as the frequency of human-specific CK8/18-positive regions relative to that of the entire examined area in the mouse liver (Tateno *et al.*, 2004), ranged from 63.7% to 86.6% (Fig. 4A). This model was found to be efficiently transduced by control HDAdV (HDΔ28E4LacZ) (Palmer and Ng, 2003) (data not shown), and so chimeric uPA/SCID mice with highly humanized livers were intravenously injected with the HL first-stage HDAdV vector.

First, GFP expression from the adenoviral backbone of the HL first-stage HDAdV in liver tissue was analyzed by flow cytometry. The results showed 7.64% ± 1.33% GFP-positive cells at 4 days postinfection and 0.21% ± 0.07% GFP-positive cells at 4 weeks postinfection. This reduction in GFP-positive hepatocytes was also confirmed by IF (Fig. 4B) and IHC (Fig. 4C).

On the other hand, βgal expression persisted for at least 4 weeks postinfection as shown by IF studies (Fig. 4D) and X-gal tissue staining (Fig. 4E). Quantitation by image analysis revealed that the percentage of βgal-positive cells increased from 16.21% ± 3.70% at 4 days, to 28.40 ± 4.92% at 4 weeks postinfection ($p = 0.0074$). The persistence of βgal expression suggested that stable integration by the second-stage LV might have occurred. To demonstrate integration of second-stage LV in human hepatocyte genomic DNA *in vivo*, nested *Alu*–lentivirus PCR was performed (Nguyen *et al.*, 2002; Serafini *et al.*, 2004). In this assay, the first round of PCR was performed using a sense primer specific for human *Alu* sequences and another primer specific for the lentiviral 5′ noncoding region as the antisense primer (*Alu*-s and 5NC2-as, respectively; Fig. 5A). As LV vectors randomly integrate at multiple sites and repetitive *Alu* sequences are scattered throughout the human genome, the first reaction generated products with variable sizes (Fig. 5B, PCR1). The second round of PCR, using nested primers within the viral LTR and the viral primer binding site, respectively ("LTR9-s" sense and "U5 PBS-as" antisense primers, as depicted in Fig. 5A), generated the expected 140-bp product from transduced liver tissues, but not from untransduced control liver (Fig. 5B, PCR1 + PCR2). Genomic DNA from transduced cells subjected only to second-round PCR amplification did not yield any signal, validating the inability of the nested primers alone to amplify any residual episomal LV sequences and confirming the requirement for first-round amplification with the *Alu*–lentivirus primers to detect integrated proviruses (Fig. 5B, PCR2). Although this is not a quantitative assay, taken together these results do demonstrate integration of the lentiviral sequences into the genome of human hepatocytes *in vivo*.

For further quantitative assessment of the percentage of cells expressing βgal from the lentivirus vector component, Q-PCR was again performed, this time using high-molecular-weight genomic DNA from each of liver tissues as the template and with primers and probe specific for the βgal gene. The Q-PCR results demonstrated that the percentage of βgal-positive cells was 13.8–56.6% at 4 weeks postinfection, correlating with the data obtained by Xgal staining (28.40% ± 4.92%) (Fig. 4E). These results indicate that *in situ* production and spread of second-stage LV had occurred in the humanized livers of chimeric mice following systemic administration of the HL first-stage HDAdV, and taken together with the above finding that the first-stage HDAdV was undetectable at 4 weeks postinfection, it is likely that βgal expression at a later time point is derived almost entirely from the second-stage LV.

To assess any potential vector-related hepatotoxicity, serum AST levels were measured and compared between HL vector-injected and control PBS-injected mice. It should be noted that the levels of serum liver enzymes in the uPA/SICD-based chimeric mouse model are generally high because of the ongoing hepatic expression of uPA, which mediates progressive destruction of murine hepatocytes and thereby allows gradual engraftment of human hepatocytes. Notably, however, there was no significant difference in the serum AST levels between HL-injected mice (272.5 ± 154.5 U/l) and PBS-treated group (453.0 ± 79.3 U/l) ($p = 0.1546$). Consistent with these findings, liver histology showed no significant difference between PBS- and HL vector-treated livers. Taken together with the serum AST levels, this indicates that the HL vector does not cause significant liver toxicity. In addition, as noted earlier, serum levels of human albumin remained at high values (>5 mg/ml) throughout these experiments, and replacement indices remained at high levels, ranging from 63.7% to 86.6% (Fig. 4A), further indicating that the HL vector does not show any selective toxicity that would alter the proportion of human hepatocytes.

Discussion

The liver has a variety of characteristics that make it a significant target for gene therapy (Ferry and Heard, 1998). As the liver is the site of essential metabolic pathways, it is involved in many inborn metabolic diseases. Moreover, because of its highly vascularized architecture and position as a portal to blood circulation, the liver can serve as a secretory organ for the systemic delivery of therapeutic proteins. Because of the fenestrated structure of its endothelium, the liver parenchyma is readily accessible to large molecules such as DNA or recombinant viruses via the blood stream. AdVs accumulate

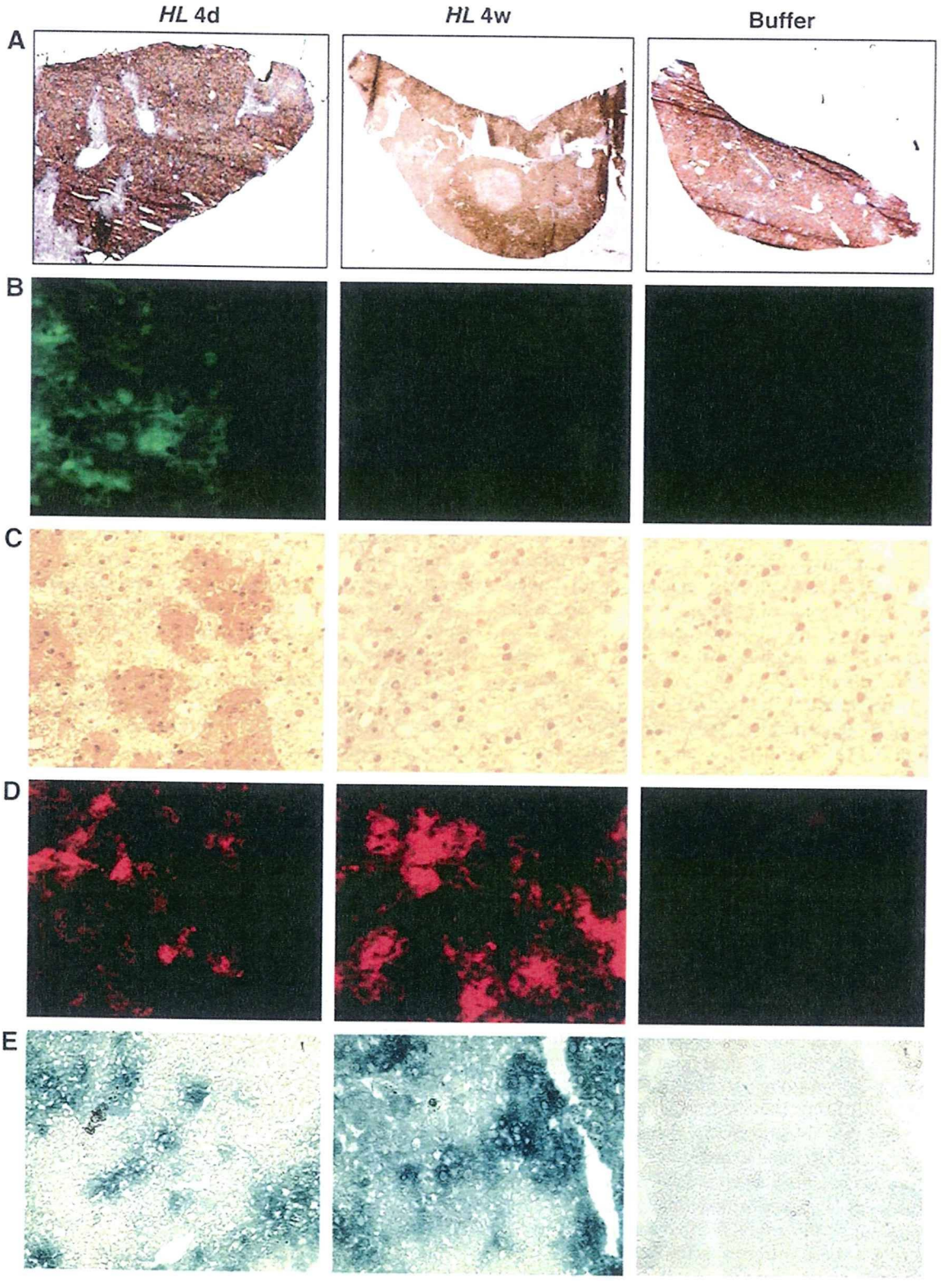

FIG. 4. *In vivo* transduction in humanized liver of the chimeric mice via HL hybrid vector system. The mice were injected with HL vector or phosphate-buffered saline (PBS) buffer. At indicated time points following HL infection, liver tissue was analyzed for GFP and βgal expression as follows: (**A**) Human CK8/18 immunostaining to determine replacement index of the mouse liver with human hepatocytes (human hepatocytes appear brown). Original magnification: 10×. (**B**) Immunofluorescence stain for GFP. Original magnification: 200×. (**C**) Immunohistochemical stain for GFP. Original magnification: 200×. (**D**) Immunofluorescence staining for βgal. Original magnification:×200. (**E**) X-gal staining. Original magnification:×100. Representative sections of each stain are shown.

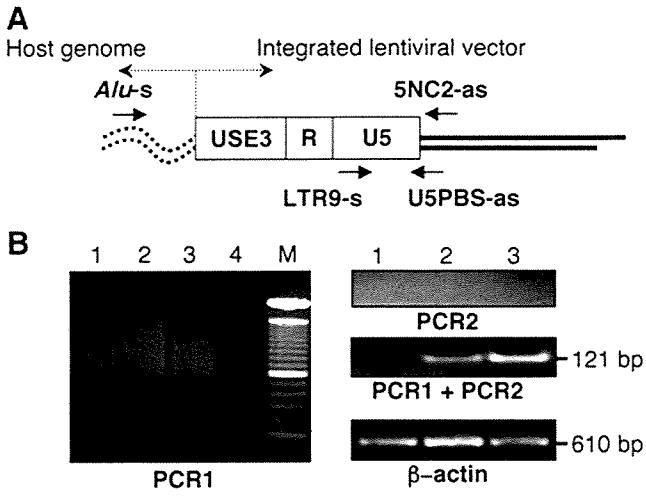

FIG. 5. Detection of integrated second-stage LV in liver tissue from chimeric mice after HL vector administration. (**A**) Design of nested polymerase chain reaction (PCR) analysis to amplify sequences spanning adjacent *Alu* repeats in the human genome (*Alu*-s and 5NC2-as) and the integrated lentiviral LTR (LTR9-s and U5PBS-as) (Nguyen *et al.*, 2002; Serafini *et al.*, 2004). (**B**) Result of nested PCR analysis: PCR1 and PCR2 correspond to the first and second rounds of nested PCR, respectively. M, 1-kb molecular mass size ladder (Invitrogen); lane 1, PBS-treated; lane 2, HL-infected, 4 days postinfection; lane 3, HL-infected, 4 weeks postinfection; lane 4, no DNA template. The 121-bp final amplification product is indicated. A 500-bp region of the human β-actin gene was amplified from the same samples as an internal control.

in the liver when injected intravenously (Kass-Eisler *et al.*, 1994; Huard *et al.*, 1995; Kubo *et al.*, 1997) and can achieve efficient hepatic gene delivery *in vivo* (Li *et al.*, 1993). The newer HDAdV system evades immune responses against transduced cells, thereby achieving long-term expression in the liver (Kim *et al.*, 2001; Oka *et al.*, 2001). However, HDAdV vectors still cannot overcome the limited duration of expression due to dilution of viral DNA as cells start to divide, a situation exacerbated if corrected hepatocytes have a selective growth advantage (Overturf *et al.*, 1996; De Vree *et al.*, 2000). Thus, the use of integrating vectors such as oncoretroviruses and lentiviruses has also been pursued.

However, hepatocytes are usually arrested in the G_0 phase of the cell cycle (Ferry and Heard, 1998), and the *in vivo* transduction efficiency of oncoretrovirus vectors is extremely low unless cell division is stimulated by growth factors or partial hepatectomy (Bosch *et al.*, 1996; Patijn *et al.*, 1998). In fact, the transduction efficiency of oncoretroviral vectors in the present uPA/SCID humanized liver model is only about 5% (Emoto *et al.*, 2005). Even though cellular mitosis is not absolutely required for lentiviral transduction, it has been reported that hepatocytes may be refractory even to lentiviral transduction unless they progress into the cell cycle (Park *et al.*, 2000), and certainly lentiviruses are incapable of efficiently transducing cells in G_0 phase, presumably because of lack of sufficient free nucleotide pools to support reverse transcription (Naldini *et al.*, 1996; Korin and Zack, 1998). As AdVs can readily infect nondividing cells (Benihoud *et al.*, 1999), it is quite advantageous to employ HDAdV as an efficient first-stage delivery vehicle for initial transient transduction of hepatocytes *in vivo*.

As the uPA/SCID chimeric mice are immunodeficient (Tateno *et al.*, 2004) and our hybrid vector is based on the HDAdV system which itself exhibits low immunogenicity (Kim *et al.*, 2001; Oka *et al.*, 2001), it might be anticipated that the HDAdV vector backbone would persist for an extended period of time in the engrafted human hepatocytes. Instead, expression of GFP in the humanized livers decreased significantly within 4 weeks after HL infection. It is possible that the toxic effects of HL-derived protein products (HIV-associated proteins and marker gene products) in the transduced cells might contribute to the activation of cell cycling in the liver; however, serum AST levels and liver histology of vector-injected animals were not significantly different from those of controls. In any case, loss of the HL-adenoviral episome would actually be advantageous to shutdown further production of the second-stage LV. To increase safety, a regulatable expression system could also be introduced into the hybrid vector to regulate LV production as reported previously (Kubo and Mitani, 2003).

Second-stage LV production *in situ* following HL vector-mediated hepatic gene transfer was assessed *in vivo* using chimeric mice in which the replacement indices indicated that the livers were almost completely repopulated with human hepatocytes. These chimeric mice have previously been shown to be a useful model for assessing the functions and pharmacological responses of human hepatocytes (Tateno *et al.*, 2004), but had never been previously employed in the evaluation of gene transfer efficiency with viral vectors.

In this humanized liver model, we observed persistent βgal expression associated with detection of integrated lentivirus sequences, despite a progressive decrease in GFP expression, suggesting that successful *in situ* production of LV had been achieved in HL-infected human hepatocytes. As noted earlier, stimulation of hepatocellular cycling after first-stage HDAdV infection might have accelerated the loss of adenoviral episomes, but may also have helped to enhance second-stage LV-mediated transduction of adjacent cells. As endogenous expression of the amphotropic envelope generally results in sequestration of the viral receptor and resistance to superinfection, it seems unlikely that cells initially transduced by the first-stage HDAdV would be reinfected with the second-stage LV. Genomic integration of the second-stage lentivirus vector was confirmed by PCR using human *Alu* and HIV LTR-specific primers. These data provide proof-of-principle for the use of the HL hybrid vector system to transduce liver parenchyma *in vivo* and for the use of the uPA/SCID mice as a model for gene delivery to human hepatocytes.

Acknowledgments

The authors thank Pedro Lowenstein for providing the FLP recombinase-based HDAdV helper system; Luigi Naldini and Didier Trono for the lentiviral packaging constructs; Stefan Kochanek for the STK plasmid; Paula Cannon for the minimal lentiviral vector; Chimoto Ohnishi for flow cytometric analysis; Maria Barcova, Celina Ngiam, and Ruth Margalit for their help during the preliminary phase of this work; and Karin Gaensler for helpful discussion. This work was supported by an NIH grant R01 CA93709 (to N.K.).

Disclosure Statement

No competing financial interests exist.

References

Benihoud, K., Yeh, P., and Perricaudet, M. (1999). Adenovirus vectors for gene delivery. Curr. Opin. Biotechnol. 10, 440–447.

Bieniasz, P.D., and Cullen, B.R. (2000). Multiple blocks to human immunodeficiency virus type 1 replication in rodent cells. J. Virol. 74, 9868–9877.

Bosch, A., McCray, P.B., Jr., Chang, S.M., Ulich, T.R., Simonet, W.S., Jolly, D.J., and Davidson, B.L. (1996). Proliferation induced by keratinocyte growth factor enhances *in vivo* retroviral-mediated gene transfer to mouse hepatocytes. J. Clin. Invest. 98, 2683–2687.

Caplen, N.J., Higginbotham, J.N., Scheel, J.R., Vahanian, N., Yoshida, Y., Hamada, H., Blaese, R.M., and Ramsey, W.J. (1999). Adeno-retroviral chimeric viruses as *in vivo* transducing agents. Gene Ther. 6, 454–459.

Chen, M., Kasahara, N., Keene, D.R., Chan, L., Hoeffler, W.K., Finlay, D., Barcova, M., Cannon, P.M., Mazurek, C., and Woodley, D.T. (2002). Restoration of type VII collagen expression and function in dystrophic epidermolysis bullosa. Nat. Genet. 32, 670–675.

Dandri, M., Burda, M.R., Torok, E., Pollok, J.M., Iwanska, A., Sommer, G., Rogiers, X., Rogler, C.E., Gupta, S., Will, H., Greten, H., and Petersen, J. (2001). Repopulation of mouse liver with human hepatocytes and *in vivo* infection with hepatitis B virus. Hepatology 33, 981–988.

De Vree, J.M., Ottenhoff, R., Bosma, P.J., Smith, A.J., Aten, J., and Oude Elferink, R.P. (2000). Correction of liver disease by hepatocyte transplantation in a mouse model of progressive familial intrahepatic cholestasis. Gastroenterology 119, 1720–1730.

Dorigo, O., Gil, J.S., Gallaher, S.D., Tan, B.T., Castro, M.G., Lowenstein, P.R., Calos, M.P., and Berk, A.J. (2004). Development of a novel helper-dependent adenovirus-Epstein-Barr virus hybrid system for the stable transformation of mammalian cells. J. Virol. 78, 6556–6566.

DuBridge, R.B., Tang, P., Hsia, H.C., Leong, P.M., Miller, J.H., and Calos, M.P. (1987). Analysis of mutation in human cells by using an Epstein-Barr virus shuttle system. Mol. Cell. Biol. 7, 379–387.

Emoto, C., Tateno, C., Hino, H., Amano, H., Imaoka, Y., Asahina, K., Asahara, T., and Yoshizato, K. (2005). Efficient *in vivo* xenogeneic retroviral vector-mediated gene transduction into human hepatocytes. Hum. Gene Ther. 16, 1168–1174.

Feng, M., Jackson, W.H., Jr., Goldman, C.K., Rancourt, C., Wang, M., Dusing, S.K., Siegal, G., and Curiel, D.T. (1997). Stable *in vivo* gene transduction via a novel adenoviral/retroviral chimeric vector [see comments]. Nat. Biotechnol. 15, 866–870.

Ferry, N., and Heard, J.M. (1998). Liver-directed gene transfer vectors. Hum. Gene Ther. 9, 1975–1981.

Graham, F.L., Smiley, J., Russell, W.C., and Nairn, R. (1977). Characteristics of a human cell line transformed by DNA from human adenovirus type 5. J. Gen. Virol. 36, 59–74.

Harui, A., Suzuki, S., Kochanek, S., and Mitani, K. (1999). Frequency and stability of chromosomal integration of adenovirus vectors. J. Virol. 73, 6141–6146.

Hofmann, W., Schubert, D., Labonte, J., Munson, L., Gibson, S., Scammell, J., Ferrigno, P., and Sodroski, J. (1999). Species-specific, postentry barriers to primate immunodeficiency virus infection. J. Virol. 73, 10020–10028.

Huard, J., Lochmuller, H., Acsadi, G., Jani, A., Massie, B., and Karpati, G. (1995). The route of administration is a major determinant of the transduction efficiency of rat tissues by adenoviral recombinants. Gene Ther. 2, 107–115.

Kass-Eisler, A., Falck-Pedersen, E., Elfenbein, D.H., Alvira, M., Buttrick, P.M., and Leinwand, L.A. (1994). The impact of developmental stage, route of administration and the immune system on adenovirus-mediated gene transfer. Gene Ther. 1, 395–402.

Katoh, M., Matsui, T., Nakajima, M., Tateno, C., Kataoka, M., Soeno, Y., Horie, T., Iwasaki, K., Yoshizato, K., and Yokoi, T. (2004). Expression of human cytochromes P450 in chimeric mice with humanized liver. Drug Metab. Dispos. 32, 1402–1410.

Kim, I.H., Jozkowicz, A., Piedra, P.A., Oka, K., and Chan, L. (2001). Lifetime correction of genetic deficiency in mice with a single injection of helper-dependent adenoviral vector. Proc. Natl. Acad. Sci. U.S.A. 98, 13282–13287.

Kochanek, S. (1999). High-capacity adenoviral vectors for gene transfer and somatic gene therapy. Hum. Gene Ther. 10, 2451–2459.

Korin, Y.D., and Zack, J.A. (1998). Progression to the G1b phase of the cell cycle is required for completion of human immunodeficiency virus type 1 reverse transcription in T cells. J. Virol. 72, 3161–3168.

Kubo, S., Kiwaki, K., Awata, H., Katoh, H., Kanegae, Y., Saito, I., Yamamoto, T., Miyazaki, J., Matsuda, I., and Endo, F. (1997). *In vivo* correction with recombinant adenovirus of 4-hydroxyphenylpyruvic acid dioxygenase deficiencies in strain III mice. Hum. Gene Ther. 8, 65–71.

Kubo, S., and Mitani, K. (2003). A new hybrid system capable of efficient lentiviral vector production and stable gene transfer mediated by a single helper-dependent adenoviral vector. J. Virol. 77, 2964–2971.

Leblois, H., Roche, C., Di Falco, N., Orsini, C., Yeh, P., and Perricaudet, M. (2000). Stable transduction of actively dividing cells via a novel adenoviral/episomal vector. Mol. Ther. 1, 314–322.

Li, Q., Kay, M.A., Finegold, M., Stratford-Perricaudet, L.D., and Woo, S.L. (1993). Assessment of recombinant adenoviral vectors for hepatic gene therapy. Hum. Gene Ther. 4, 403–409.

Lieber, A., He, C.Y., Meuse, L., Schowalter, D., Kirillova, I., Winther, B., and Kay, M.A. (1997). The role of Kupffer cell activation and viral gene expression in early liver toxicity after infusion of recombinant adenovirus vectors. J. Virol. 71, 8798–8807.

Lieber, A., Steinwaerder, D.S., Carlson, C.A., and Kay, M.A. (1999). Integrating adenovirus-adeno-associated virus hybrid vectors devoid of all viral genes. J. Virol. 73, 9314–9324.

Mariani, R., Rutter, G., Harris, M.E., Hope, T.J., Krausslich, H.G., and Landau, N.R. (2000). A block to human immunodeficiency virus type 1 assembly in murine cells. J. Virol. 74, 3859–3870.

Mercer, D.F., Schiller, D.E., Elliott, J.F., Douglas, D.N., Hao, C., Rinfret, A., Addison, W.R., Fischer, K.P., Churchill, T.A., Lakey, J.R., Tyrrell, D.L., and Kneteman, N.M. (2001). Hepatitis C virus replication in mice with chimeric human livers. Nat. Med. 7, 927–933.

Naldini, L., Blomer, U., Gallay, P., Ory, D., Mulligan, R., Gage, F.H., Verma, I.M., and Trono, D. (1996). *In vivo* gene delivery and stable transduction of nondividing cells by a lentiviral vector. Science 272, 263–267.

Nguyen, T.H., Oberholzer, J., Birraux, J., Majno, P., Morel, P., and Trono, D. (2002). Highly efficient lentiviral vector-mediated